

Designing Steel Joist Seats Subjected to Rollover Forces

By

Mitchel Stipek

A thesis submitted to the Department of Civil Engineering,

Cullen College of Engineering

in partial fulfillment of the requirements for the degree of

Masters of Science

in Civil Engineering

Chair of Committee: Dr. Abdeldjelil Belarbi

Committee Member: Dr. Reagan Herman

Committee Member: Dr. Mina Dawood

University of Houston

May 2020

Copyright 2020, Mitchel Edward Stipek

Abstract

The mechanisms governing the response of steel joist seats subjected to rollover forces were identified through physical testing of fifteen specimen pairs and the applications of concepts from Fisher et al. (2002) and Green and Sposito (2002). The experimental test method was developed based on the field observations to more closely resemble actual conditions of steel joist seats in buildings. In doing so, it was observed that the response of joist seats subjected to rollover can be separated into two phases: elastic and inelastic. In both phases, it was observed that the shape of the yield line produced on the bearing seat did not vary with the thickness of the material, as was observed by Green and Sposito (2002), but was consistent across all bearing seat sizes and thicknesses. Applying the yield line concepts from Green and Sposito (2002) and the rollover statics from Fisher et al. (2002) to this new yield line geometry produced a plausible method for predicting joist seat rollover capacity. With more extensive testing across a wider range of bearing seat thicknesses and sizes, the observations from this testing could produce a simple analytical model for predicting rollover capacity of joist seats for industry's use.

Table of Contents

Abstract.....	iii
Table of Contents.....	iv
List of <i>Tables</i>	vi
List of <i>Figures</i>	viii
Chapter 1 - Introduction	1
1.1 Introduction to Steel Joists	1
1.2 Steel Industry Pricing.....	2
1.3 Design and Fabrication of Steel Joists.....	3
1.4 Erection of Steel Joists	8
1.5 Specification of Steel joists	9
1.6 Open Web Steel Joists and Lateral Systems	11
1.7 Typical Joist Seats.....	16
1.8 Rollover Forces on Joist Seats	21
1.9 Scope and Objective.....	22
Chapter 2 – Literature Review	23
2.1 Introduction.....	23
2.2 Resistance Based on Yield Strength – Fisher et al. (2002)	23
2.3 Resistance Based on Ultimate Strength – Fisher et al. (2002).....	26
2.4 Determining Strength Through Testing	28
2.5 Behavior of Open Web Steel Joist Seats Subjected to Lateral Loads.....	31
2.5.1 Doyle (2010) Findings	34
2.6 Green and Sposito (2002) Yield Line Theory	36
2.7 Applying the Green and Sposito (2002) Yield Line Theory	37
2.8 Internal Stiffness vs. Bearing Seat Capacity	39
2.9 Summary	42
Chapter 3 – Methods	43
3.1 Introduction.....	43
3.2 Test Setup.....	43
3.3 Instrumentation	49

3.4	Data Acquisition System.....	51
3.5	Specimen Details	51
3.6	Test Procedure	54
Chapter 4 – Results		56
4.1	Introduction.....	56
4.2	Qualitative Test Results.....	56
4.3	Individual Specimen Results.....	58
4.3.1	Test Configuration 20250	58
4.3.2	Test Configuration 20188	59
4.3.3	Test Configuration 20163	61
4.3.4	Test Configuration 15155	62
4.3.5	Test Configuration 15113	62
4.4	Quantitative Results	63
Chapter 5 – Discussion.....		67
5.1	Introduction.....	67
5.2	Effects of Fabrication Quality.....	67
5.3	Overview of Statics.....	68
5.4	Mechanisms	70
5.5	Performance in Each Stage	74
5.5.1	The Elastic Stage	74
5.5.2	The Inelastic Stage	81
5.6	Summary	83
Chapter 6 – Summary and Conclusions		85
6.1	Introduction.....	85
6.2	Summary of Existing Body of Knowledge and Design Methods	85
6.3	Conclusions.....	86
6.4	Location of the Bearing Weld.....	87
6.5	Future Research	87
References		89

List of *Tables*

Table 2-1 - Minimum Bearing Weld Lengths	34
Table 3-1 - Properties of the Specimens to be Tested	53
Table 4-1 - First Yield and Ultimate Loading Recorded from Experiments	65
Table 4-2 - Variation of Modulus of Elasticity, First Yield and Ultimate Loads and Displacements from Experimental Data	66
Table 5-1 - Comparison of Likely Locations for the Compression Reaction	75
Table 5-2 - Deviation of Observed First Yield Strength vs. First Yield Strength Estimated with Application of Green and Spath (2002)	77
Table 5-3 - Experimental vs. Theoretical First Yield Capacity Utilizing Adjusted Yield Line Model	80
Table 5-4 - Experimental vs. Theoretical Ultimate Capacities	83

List of *Figures*

Figure 1-1 - Large Fabricated Trusses Used in the Dallas Cowboys' AT&T Stadium.....	2
Figure 1-2 - Steel Joist Used In a Warehouse Roof.....	2
Figure 1-3 - Typical Rod Joist With Double Angle Chord and Continuous Bent Rod Webs	3
Figure 1-4 - Joist Rigging Table.....	4
Figure 1-5 - 3 Steel Joists "Stacked" Together After Rigging	5
Figure 1-6 – Joists Stacked and Laid Sideways Allowing Simultaneous Preparation and Welding.....	6
Figure 1-7 - Joists Dip Painted in a Nine Joist Bundle	8
Figure 1-8 - Typical Joist Unstiffened Seated Connection	9
Figure 1-9 - Underslung Steel Joist With Center of Mass Below Bearing Elevation	9
Figure 1-10 - Conventional Steel Construction - Steel Deck, Steel Joists, and Wide Flange Beams and Columns	11
Figure 1-11 - Lateral Wind Load Carried Through the Structure to the Ground	12
Figure 1-12 - Lateral Loading from Diaphragm Passes Through Joist Seats to Primary Framing Element.....	13
Figure 1-13 - Typical Joist Seat With Rollover Force Applied From Diaphragm	14
Figure 1-14 - Typical Joist Seat With and Without Seat Stiffeners	15
Figure 1-15 - Generic Joist Seat Idealized as Two Channels and a Rigid Element	17
Figure 1-16 - Typical Lapped Joist Seat	17
Figure 1-17 - Typical Butted Joist Seat.....	18
Figure 1-18 - Typical Gapped Joist Seat	19
Figure 1-19 - Typical Gapped Seat With Sloped Top Chord.....	19
Figure 1-20 - Typical Bent Plate and 3-Plate Saddle Seats	20
Figure 1-21 - Typical T-Plate and Back to Back Seats.....	21
Figure 1-22 - Generic Joist Subjected to a Rollover Force	22
Figure 2-1 - Joist Seat Resisting Rollover Force	24
Figure 2-2 - Effective Angle Width	25
Figure 2-3 - Seat Failure Mode.....	27
Figure 2-4 - Load Arrangement for Vulcraft Testing.....	29
Figure 2-5 - Canting Joist Seat.....	32
Figure 2-6 - Racking Joist Seat.....	32
Figure 2-7 - Field Examples of a Rollover Failure.....	33
Figure 2-8 - Test Setup With Two Joist Seats Connected by a Rigid Element and Loaded Simultaneously.	33
Figure 2-9 - Simplified Yield Line of Bearing Angles Subjected to Uplift Forces.....	36
Figure 2-10 - Applying the Yield Line Theory from Green and Sposito (2002) to Joist Seats Subjected to Rollover Forces	38

Figure 2-11 - Two Weld vs. Four Weld Lapped Configuration.....	40
Figure 2-12 - Performance of "2-Weld" vs. "4-Weld" Configurations Subjected to Rollover	40
Figure 2-13 - Deflection Assemblies of "2-Weld" and "4-Weld" Configurations.....	41
Figure 3-1 - Test Specimen.....	44
Figure 3-2 - The Test Table Used to Conduct the Experiments Shown Loaded with a Specimen	44
Figure 3-3 - Test Frame Shown Holding the Other Elements Before Installing Stiffeners	45
Figure 3-4 - Specimen Platform Shown Loaded With a Specimen and the Bearing Plate Stiffeners Attached.....	46
Figure 3-5 - Hydraulic Ram Uplift Before Modification of the Test Setup.....	47
Figure 3-6 - Load Transfer Frame Used to Carry Load from the Hydraulic Ram to the Specimen	48
Figure 3-7 - Added Stiffener Bars Preventing Warping of Bearing Plate.....	49
Figure 3-8 - Load Cell Located Between the Hydraulic Ram and the Load Transfer Frame	50
Figure 3-9 – String Potentiometer on the Specimen Platform.....	50
Figure 3-10 - Standard Lapped Seat Configuration	52
Figure 3-11 - Safety Weld on Lapped Configuration Joist Seats.....	53
Figure 4-1 – Test 15155-A Yield Line Formed on the Tension Side Bearing Angle.....	57
Figure 4-2 – Bearing Weld Tear on 15155-A.....	58
Figure 4-3 - Configuration 20250 Load Displacement Curve.....	59
Figure 4-4 - Configuration 20188 Load Displacement Curves	60
Figure 4-5 - Specimen 20188-C After Failure.....	60
Figure 4-6 - Configuration 20163 Load Displacement Curves	61
Figure 4-7 - Configuration 15155 Load Displacement Curves	62
Figure 4-8 - Configuration 15113 Load Displacement Curves	63
Figure 4-9 - Example of an Modulus of Elasticity Line Matched to a Load Displacement Curve to Determine the First Yield Point	64
Figure 5-1 - Idealized Sketch of Joist Seat vs. the Manufactured Joist Seat.....	68
Figure 5-2 - Typical Statics of a Steel Joist Seat Subjected to Rollover Forces	69
Figure 5-3 - The Two Mechanism Stages Shown on Experimental Data	70
Figure 5-4 - Typical Observed Yield Line During Testing.....	71
Figure 5-5 - Idealized Yield Line Based on Green and Sputo (2002).....	72
Figure 5-6 - Joist Seat After Failure due to Lateral Rollover Forces	73
Figure 5-7 - Seat Appearance After Formation of Plastic Hinges in All Elements.	73
Figure 5-8 - Applying Green and Sputo (2002) Yield Line to Joist Seats Subjected to Rollover.....	75
Figure 5-9 - Bearing Seat Thickness vs. Elastic Limit.....	77
Figure 5-10 - Yield Line Based on Experimental Data.....	78
Figure 5-11 - Tension Component Forms as Bearing Angle Deforms.....	81

Chapter 1 - Introduction

1.1 Introduction to Steel Joists

Trusses are very common in modern construction because they offer superior weight to strength ratios compared to wide flange beams and other rolled sections. Furthermore, engineers choose to use steel trusses due to their greater strength to weight ratio in both compression and tension, as opposed to wood and concrete trusses. Steel trusses fall into two main categories: fabricated trusses, and open web steel joists, just called joists.

Fabricated trusses are built in pieces by a steel fabricator and assembled at the job site before erection. Fabricated trusses are typically used in projects with large spans, high loading, or very special conditions when it is not practical, or possible, to use other products. Common examples of uses for fabricated trusses are large stadium roofs and industrial utility structures like those shown in Figure 1-1. Because fabricated trusses are designed and built specifically for individual job sites and loading conditions, these trusses can be built using a wide variety of steel shapes, from wide flange beams to single angles depending on design requirements.



Figure 1-1 - Large Fabricated Trusses Used in the Dallas Cowboys' AT&T Stadium

Like fabricated trusses, joists are also custom-made to meet the specific loading conditions of the job, but are more commonly used because they are simpler and less expensive to design, build and erect. They are used in projects that use conventional steel construction such as warehouses, schools, and stores like those shown in Figure 1-2.

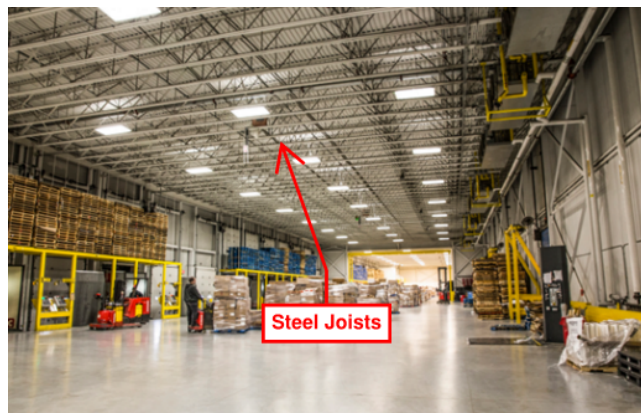


Figure 1-2 - Steel Joist Used In a Warehouse Roof

1.2 Steel Industry Pricing

Products in the steel industry are typically sold by the ton, with adjustments for special costs. A typical fabricated truss produced by a steel fabrication shop will cost

\$2,200 – \$2,800 a ton, while a steel joist built by a joist fabricator with the same capabilities will cost \$1,100 - \$1,400 a ton. For reference, a wide flange beam with the same capabilities built by a steel fabricator would cost \$1,700 - \$2,000 a ton. Steel joists are considerably less expensive than fabricated trusses and wide flange beams due to their simplicity and to standardization in both design and fabrication of the joist.

1.3 Design and Fabrication of Steel Joists

Joists are typically built using double angle chord members, along with single member hot- or cold-rolled shapes, commonly called “webs,” between the chord members. A common example of this is a “rod joist”, shown in Figure 1-3, which is built with a continuous bent round bar for webs between the double angle chords.

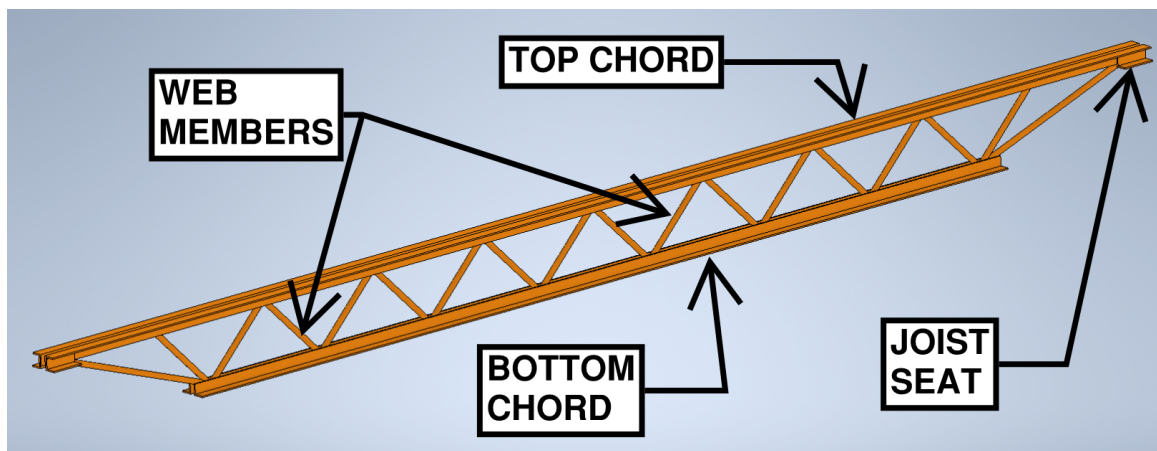


Figure 1-3 - Typical Rod Joist With Double Angle Chord and Continuous Bent Rod Webs

The standardization of joist design allows the fabrication process to be separated in distinct, specialized, and repeatable operations. Joist fabrication resembles a continuous assembly line, as compared to fabricated trusses and beams that are built one at a time.

The fabrication process is broken into five distinct operations: “cut-out”, “rigging”, “welding”, “inspection”, and “painting”.

In the “cut-out” operation, all components required for the assembly of the joist are cut to length and staged for “rigging”. During the “rigging” process, all components are “rigged”, or assembled, by a team of workers on a specialized table using clamps or tack welds. The table, seen in Figure 1-4, is set up with guides so workers can quickly place the components without making any measurements.



Figure 1-4 - Joist Rigging Table

When a joist is fully rigged, it is rolled out of the table, onto a roller bed, and stacked in groups of three or four with other completed joists on their sides, as seen in Figure 1-5. This stacking is very important to later parts of the fabrication process and is only possible because of the joist design. The double angle chords can be nested together unimpeded by the single member webs between them.

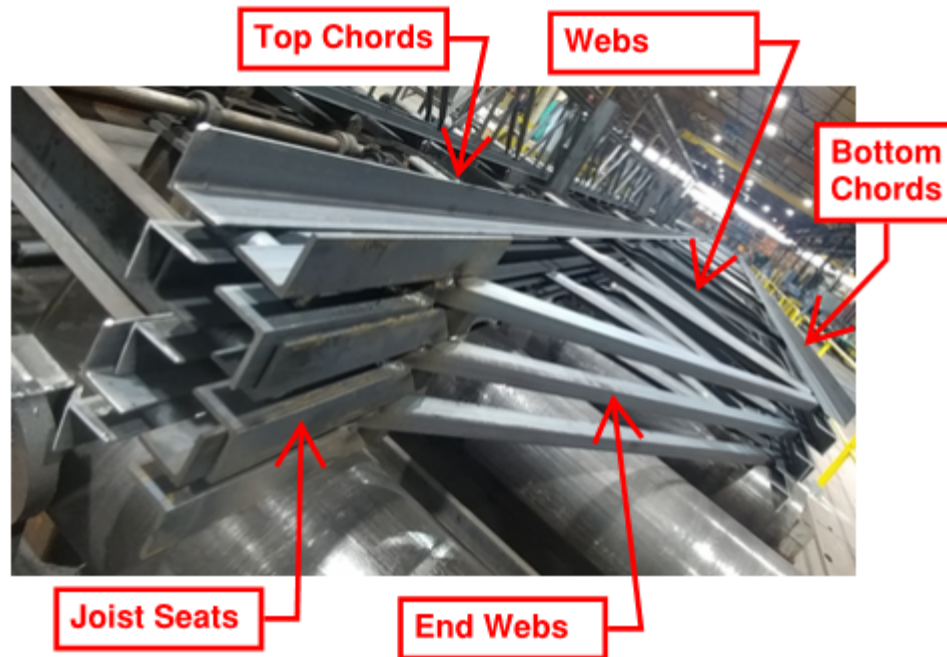


Figure 1-5 - 3 Steel Joists "Stacked" Together After Rigging

The rigging operation is completed within ten to twenty seconds with small rod joists, between ten and twenty feet long, and can be repeated continuously. Therefore, it is the job of the cut-out operation to keep ahead of the rigging operation, with the components of many joists staged so that the workers in the rigging operation do not have to wait for new material.

Once the joists are stacked, they move to the “welding” process, where teams of welders apply all of the final structural welds. Welding is the slowest part of the fabrication process because it must be done very carefully to ensure acceptable weld quality. Welding requires substantial preparation time between welds as the welders must have very precise access to the joints that are going to be welded; and most welds can only be performed from specific directions. For example, a typical fillet weld needs to be performed from above on a flat and level surface. To accomplish this, welded

structural members typically need to be flipped and spun numerous times for a welder to get such access to all required joints. Due to their weight, the process of flipping a structural member requires the use of a crane or other special equipment, making it a very slow process. In the fabrication industry, a measure of the productivity of a welding operation is the amount of time a welder spends actually welding versus the amount of time they spend preparing a joist to be welded by flipping or moving a member. In a typical steel fabrication operation, a welder will spend only 40% of their time welding, while the rest is devoted to preparation.

The configuration of the joists, with single member webs between double angle chords, allows them to stack in groups of three or four, allowing them to be welded with much less preparation time. Several joists can be welded at a time from the top or the bottom without unstacking them, meaning the preparation for those joists can be done simultaneously. Additionally, the stacks of joists are laid on their sides, as seen in Figure 1-6, so that one team can weld the top while another team welds the bottom at the same time.



Figure 1-6 – Joists Stacked and Laid Sideways Allowing Simultaneous Preparation and Welding

Stacking the joists and welding in this manner means the joists only need to be flipped one time to be fully welded. When welding stacked joists, the welding team spends almost 90% of their time welding, resulting in a substantial increase in productivity compared to other products, including joists that cannot be stacked.

After welding is complete, the stacks of joists continue down the roller bed to the “inspection” operation. During the inspection process, the joists are visually inspected to ensure the joists were fabricated correctly and meet all quality standards. If any corrections are required, the adjustments are made prior to the joists continuing down the roller bed to the “painting” operation.

During the painting process, several stacks of joists are combined into bundles of eight to twelve joists and then dipped into a tank containing rust-inhibiting paint, as seen in Figure 1-7, which protects the joists until they arrive and are erected at a job site. This bundling and painting process is much quicker than traditional steel fabrication, where only one member can be spray-painted at a time. In this manner, the entire bundle of joists can be painted in the time it would take to paint a single prefabricated truss or beam. However, this bundling and painting process is only an advantage when the joists are able to stack.



Figure 1-7 - Joists Dip Painted in a Nine Joist Bundle

When painting is complete, bundles are stacked on trailers for shipping. When stacking the joists on trucks, operators must take into consideration the truck's weight and space capacities. Because joists have a low weight to strength ratio, they are relatively light for the space they occupy. Due to this lower weight, joists commonly reach the truck's space capacity, called "cubing out," before exceeding the truck's weight capacity. Joists that can be stacked take considerably less space on the truck bed, which allows more joists to be loaded on each truck, thereby reducing shipping costs.

1.4 Erection of Steel Joists

Steel joists are much easier and faster to erect compared to other structural members. Steel joists are underslung, bearing on other structural members with unstiffened seated connections on their top chords, as seen in Figure 1-8. Being underslung means the center of mass of the truss assembly is below the connection

point, as shown in Figure 1-9. Because of this, the joist is inherently stable and can be set in place by a crane and released with little or no physical connection being made. This process is much faster than the placement of beams or prefabricated trusses, as those members require large bolted or welded connections that must be lined up and assembled before they can be released from the crane.

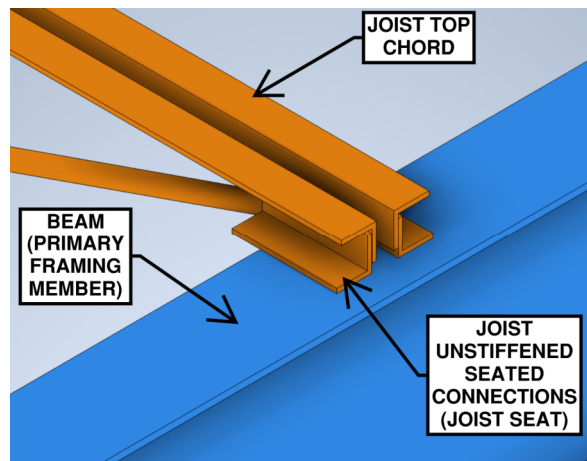


Figure 1-8 - Typical Joist Unstiffened Seated Connection

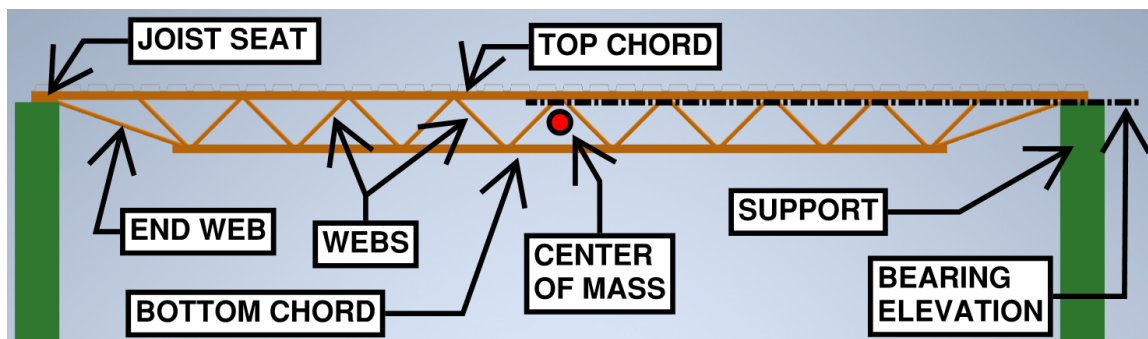


Figure 1-9 - Underslung Steel Joist With Center of Mass Below Bearing Elevation

1.5 Specification of Steel joists

Steel joists are inexpensive to fabricate and erect, but their standardization also makes them very easy to specify and design. Joists are specified by a designation that correlates to the relative properties of that joist. These joist designations are made up of

three parts: a number, a letter series, and another number, for example “30K7”. The first number represents the depth, in inches, of the joist. The letters represent the joist series, which determines a set of requirements the joist is designed by. “K” series joists, called “short span” joists, are smaller, lighter joists, typically between ten and thirty inches deep and less than sixty feet long. “LH” series joists, called “long span” joists, have additional design requirements, can be between eighteen and sixty inches deep, and up to one hundred and twenty feet long. There are a few other less common series such as “KCS” and “DLH”, and many retired series such as “J” series or “H” series, but the “K” and “LH” series are the most common. The final number in the joist designation is a relative loading number, where a higher number represents a larger loading capacity. For example, a 30K9 would have a higher capacity than a 30K7.

The chief engineer for a project, legally called the “Engineer of Record” or “Specifying Professional”, is able to use standard loading tables published by the Steel Joist Institute, the governing body for steel joist design, to select a joist designation. The joist manufacturer is then responsible for designing a joist that fits all the requirements of the joist designation selected by the engineer. This standardization of joists through designations makes the design process much quicker and more efficient when compared to other products, such as prefabricated trusses, which must be fully designed by the engineer.

1.6 Open Web Steel Joists and Lateral Systems

Joists are only one part of the roof system and are typically used as secondary framing components. Joists directly support the roof or floor deck, and are also supported themselves by primary framing components such as beams or joist girders, a primary framing application of open web steel joists. The distinction between primary and secondary members is that secondary members frame into primary members, and the primary members then frame into columns or other vertical supports. This can be seen in Figure 1-10. Note that a section of the deck is cut to show the joist bellow. Additionally, secondary members are not typically involved in the building's lateral systems used to resist lateral loads such as wind or earthquakes.

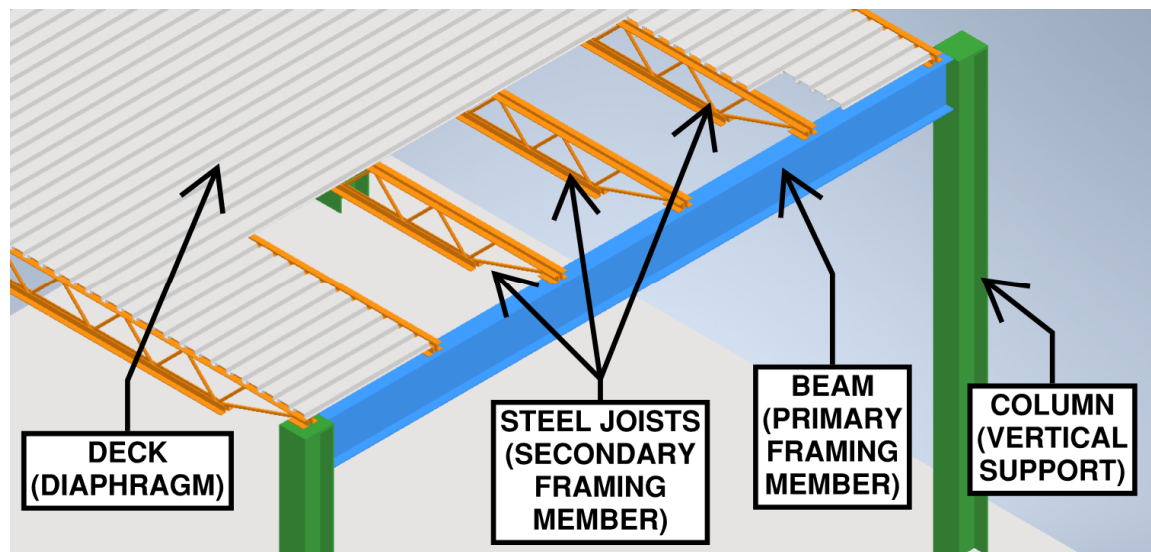


Figure 1-10 - Conventional Steel Construction - Steel Deck, Steel Joists, and Wide Flange Beams and Columns

However, secondary members do support the roof and floor deck, which is typically a corrugated steel deck in steel construction. This deck is important because it supports the finished roof or floor, carrying loads to the joists, and also contributes to the lateral

system. Deck acts as a “diaphragm” to carry lateral loads applied at various locations throughout the building to the primary members which carry the loading to columns or shear walls. These columns or shear walls take the lateral loading to the ground as seen in Figure 1-11.

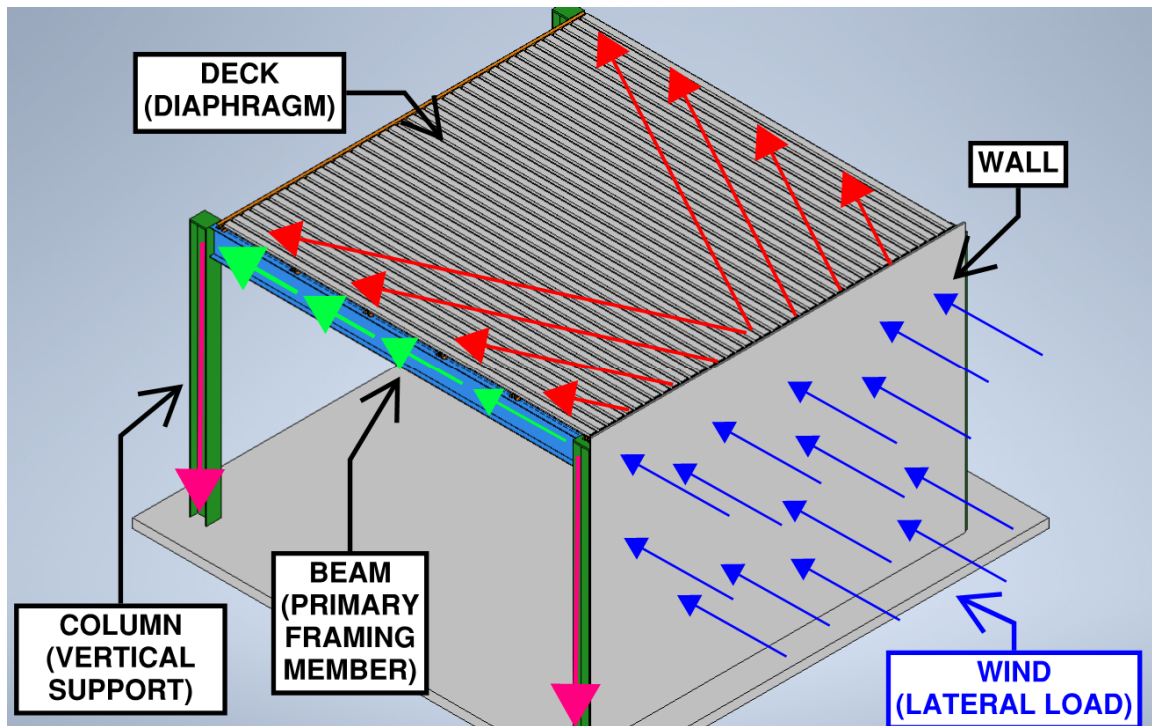


Figure 1-11 - Lateral Wind Load Carried Through the Structure to the Ground

However, with conventional steel construction using joists, the deck is not directly connected to the primary framing members. Therefore, any lateral loading traveling through the diaphragm must be transferred through the joists, or a separate reinforced member called a “shear collector,” to reach the primary framing members. As seen in Figure 1-12, if shear collectors are not used, this load must be transferred laterally through the joist’s seated connection.

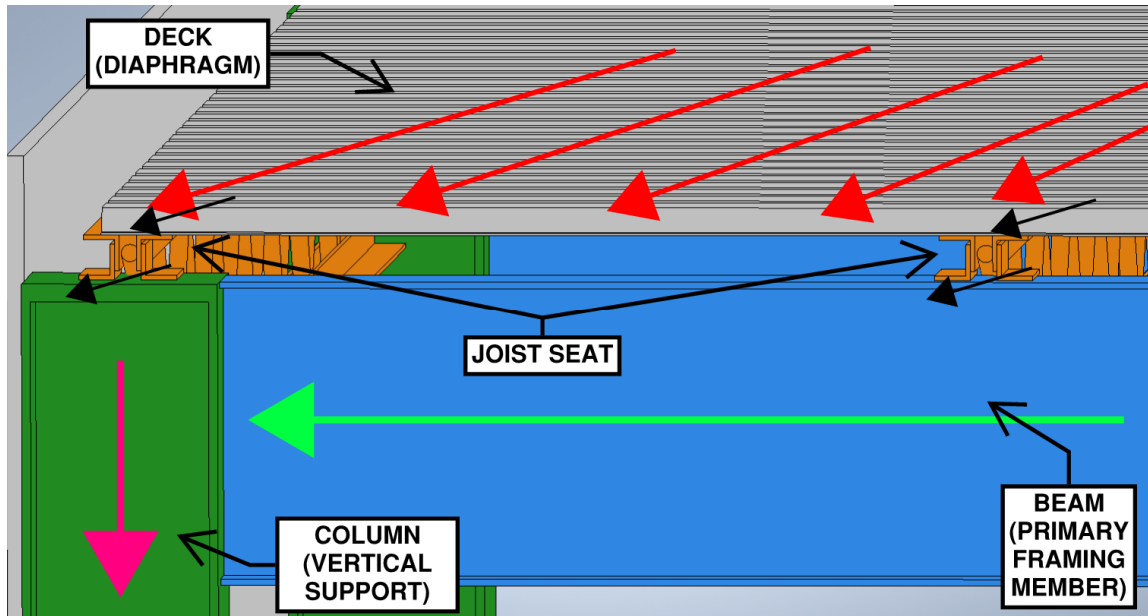


Figure 1-12 - Lateral Loading from Diaphragm Passes Through Joist Seats to Primary Framing Element

The unstiffened seated connections of joists are very efficient to build in the fabrication process, are very effective at bringing the gravity loads of the joist to the support, and are very fast to erect as mentioned previously. However, these seated connections are not ideal for lateral loading from the steel deck in this manner.

Analyzing the cross section of a typical joist seat in Figure 1-13, it can be seen that these seats resemble built up double channels, and the lateral force from the steel deck is an out-of-plane load along its weakest axis. In industry, a lateral load applied to the joist seat in this manner is called rollover. Not only is it readily apparent that the joist seats are not ideally suited for carrying rollover loads, but analyzing the strength of joist seats loaded in this manner is very difficult as well. In order to overcome this challenge, alternatives methods of transferring the lateral load from the deck to the primary members have been developed and utilized throughout the steel industry.

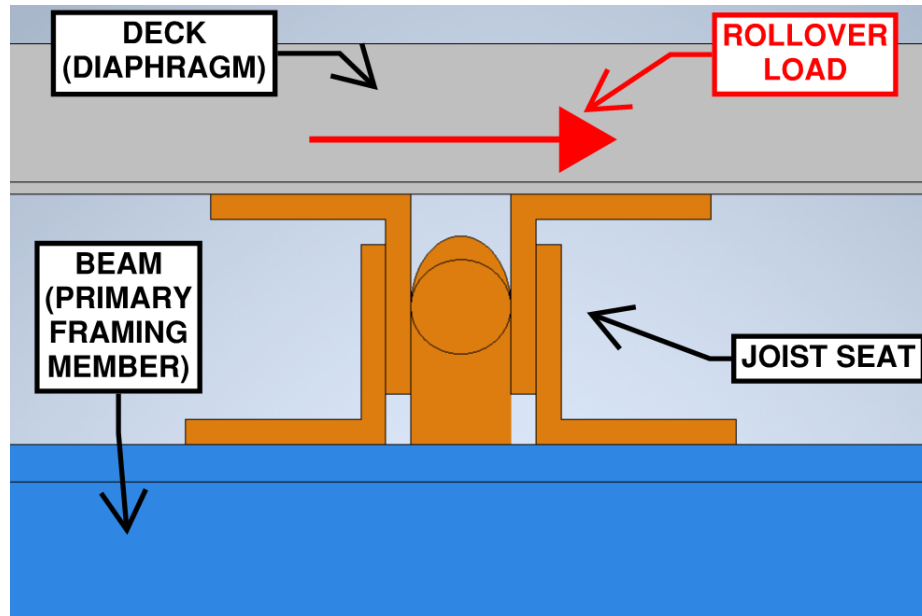


Figure 1-13 - Typical Joist Seat With Rollover Force Applied From Diaphragm

There are two alternatives to a generic joist seat, like that shown in Figure 1-13, being used to transfer this rollover force. The first is to use additional framing members, called shear collectors, to carry the load instead of the joist seat. These shear collectors are typically steel tubes that are placed in between the joist seat, on the primary framing members, oriented in line with the lateral load from deck. Because of their stiffness, shear collectors are very effective at transferring the load away from the joist seat. However, there are a few drawbacks to utilizing shear collectors, primarily associated with the cost to fabricate the joist. The steel tubes used for shear collectors are very expensive, costing about \$2,200-\$2,500 a ton, and while the individual collectors will only weigh 30-70 pounds, there will be one collector for every joist on the project, regardless of size. Using an average sized joist as an example, a 30K7, which is 30 inches deep and 50 feet long, weighs roughly 350 pounds. Most jobs require an average of one shear collector per joist, which adds up to twenty percent additional

weight to each joist, and thereby increases the cost of each joist. Additionally, this doubles the piece count that must be installed by the erector, in effect doubling the placement time of secondary members.

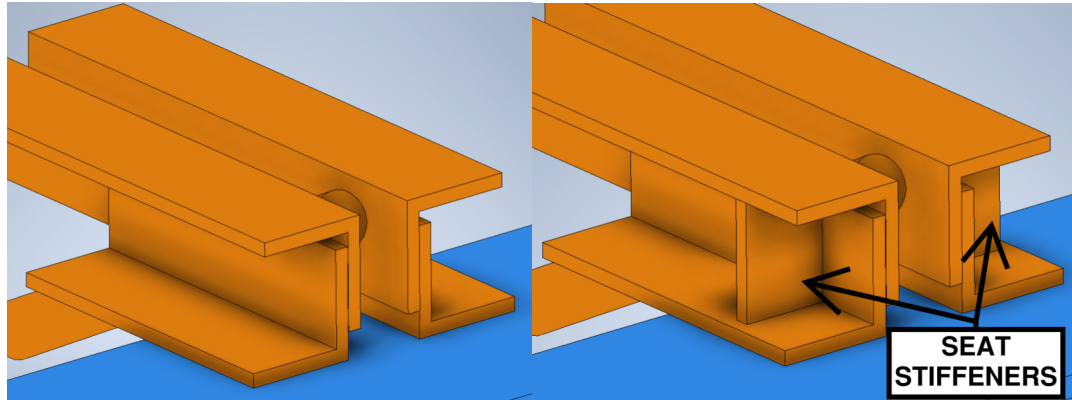


Figure 1-14 - Typical Joist Seat With and Without Seat Stiffeners

The other alternative is to install seat stiffeners in the typical joist seat, as shown in Figure 1-14. These stiffeners can be analyzed to carry the rollover force in simple shear, making design very simple. However, seat stiffeners have a significant impact on the fabrication process because they prevent the joist from being stacked. Aside from the need to have access for welding, the seat stiffeners physically prevent the joists from being nested at the seat, making it impossible to create the stacks. As mentioned previously in this chapter, the stacking of joists is very important for the productivity of the fabrication process and improving the shipping efficiency. Losing the ability to stack joists adds roughly \$25-\$50 per joist of additional cost due to additional fabrication time alone, regardless of joist size. Using a 30K7 joist as an example, this piece weighs 350 pounds and costs \$220 (assuming an average cost of \$1,250 per ton). Adding the seat stiffener results in a minimum increase in costs of ten percent for fabrication alone. This

cost would be even further magnified on smaller joists. On an average 10K1, which is ten inches deep, roughly fourteen feet long, weighing only 50 pounds and costing only \$35 per joist, seat stiffeners could mean doubling the cost of each joist.

In the interests of simplification and reducing fabrication costs, it would be ideal to improve the understanding of the strength and abilities of the typical joist seats to carry these rollover forces and design them so that shear collectors and seat stiffeners are not required.

1.7 Typical Joist Seats

The “generic” joist seat can be idealized as two channels separated by a semi rigid element as seen in Figure 1-15 with labeled components. While most joist seats have similar components and resemble this generic joist seat, there are many different configurations that can be used for different framing scenarios. For all joist seats, the bearing depth, or seat height “ h ” is the distance from deck bearing elevation to joist bearing elevation, or the top of the top chord to the bottom of the bearing seat. The width of the joist seat “ w_e ” is the distance between the horizontal toes of each bearing angle. This dimension can and often is different than the top chord width, measured in the same way. The joist seat is welded to the support by two, eight-inch fillet welds, two and a half inches long, which are located at the toe of each of the bearing angles.

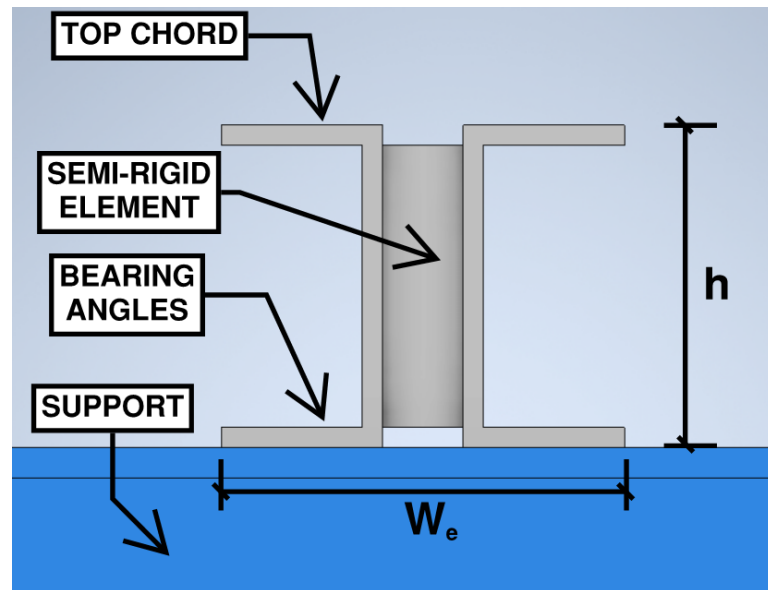


Figure 1-15 - Generic Joist Seat Idealized as Two Channels and a Rigid Element

The most common of these configurations is the “lapped” seat, which uses two bearing angles lapped and welded directly to the top chord, as seen in Figure 1-16, with the end rod acting as the semi-rigid element. Lapped seats are most common because they are extremely simple and are very easy to fabricate. Lapped seats also require the fewest pieces because the end web acts as the semi-rigid element. However, lapped seats can only be used with bearing depths less than three and a half inches, as the bearing angles must have sufficient overlap on the top chord.

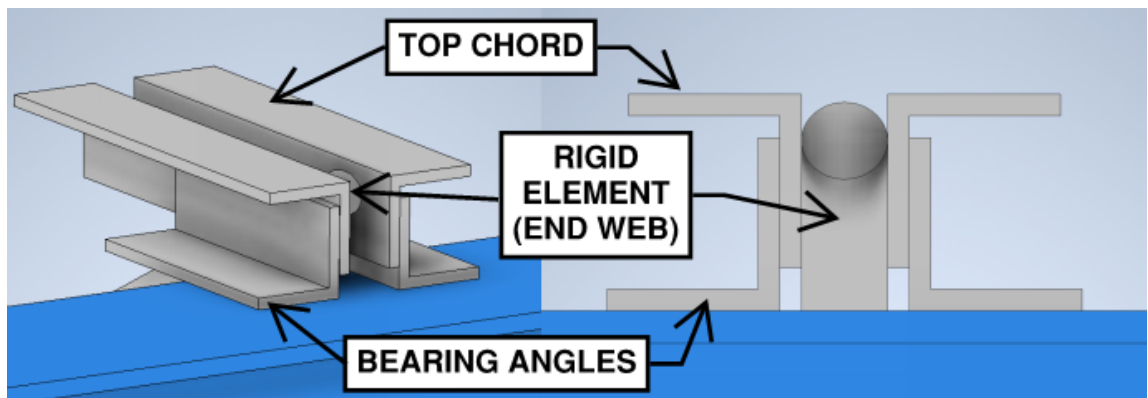


Figure 1-16 - Typical Lapped Joist Seat

Butted seats use two bearing angles butted with the top chord and connected by a vertical peg, typically a round bar as seen in Figure 1-17. Butted seats are easy to fabricate because they do not require any measurements since the bearing angles are butted to the top chord. However, butted seats are only possible in conditions where the required top chord angles and bearing angles happen to equal the bearing depth.

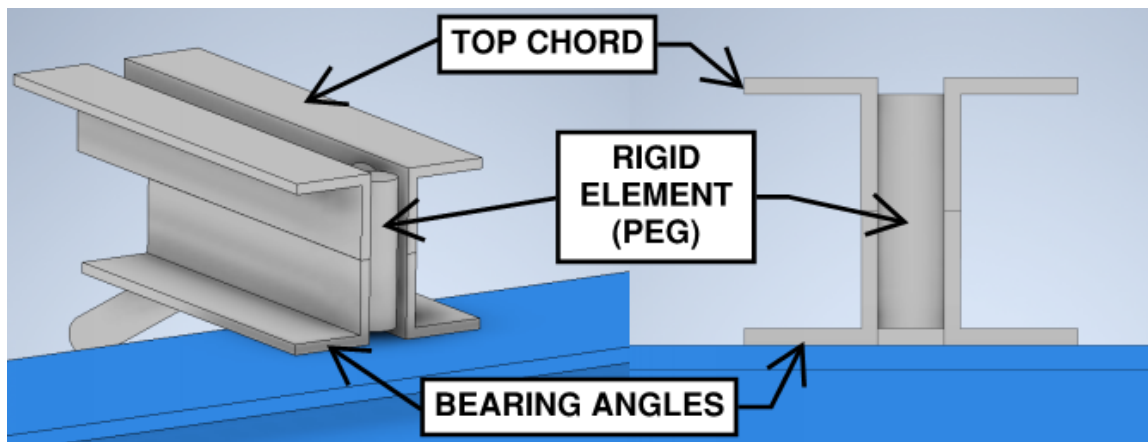


Figure 1-17 - Typical Butted Joist Seat

Gapped seats are similar to butted seats in that they consist of two bearing angles and a vertical peg. However, rather than being directly butted to the top chords, there is a gap between the bearing angles and the top chord, as seen in Figure 1-18. Gapped seats are common when there is a large bearing depth and are convenient because they allow the seat to be sloped. When a roof is sloped, the joist seat still requires level bearing, and this is typically addressed by sloping the joists seat as seen in Figure 1-19. However, gapped seats are very difficult to fabricate as the worker in the rigging operation is required to make many measurements to ensure that they are installed correctly.

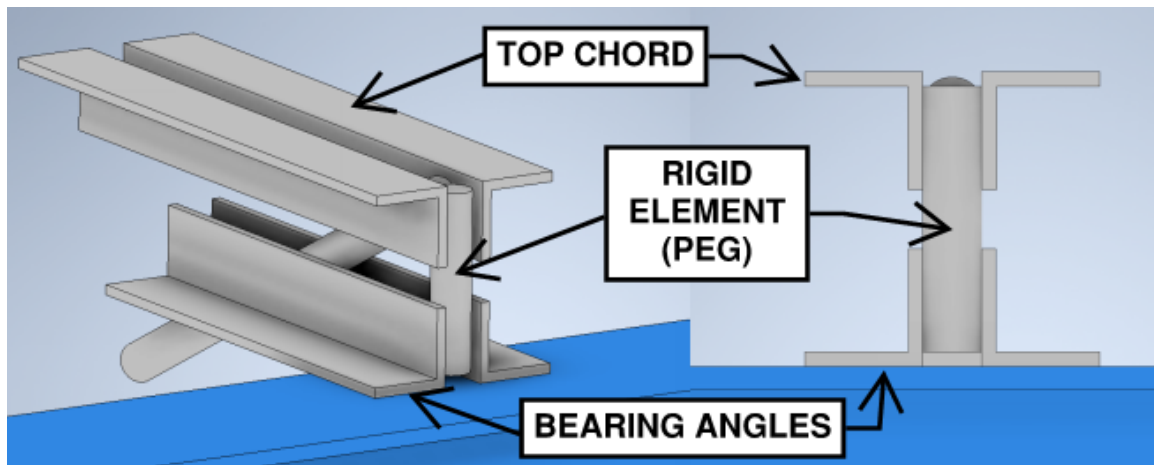


Figure 1-18 - Typical Gapped Joist Seat

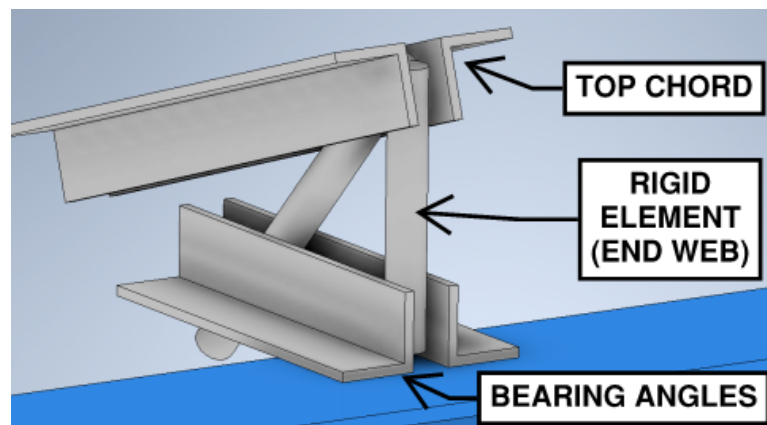


Figure 1-19 - Typical Gapped Seat With Sloped Top Chord

To improve on the production efficiency of sloped seats, it is common to use saddle seats, which are prefabricated during the cut-out process with plates such that they can be installed by the rigging operation without making any measurements. There are two different kinds of saddle seats: bent plate saddles and three plate saddles, as seen in Figure 1-20. Saddles are much faster for fabrication, but are very specialized and not as capable of carrying large or specialized loads as other seat configurations. This is particularly true of rollover forces, which saddle seats have essentially zero strength to resist.

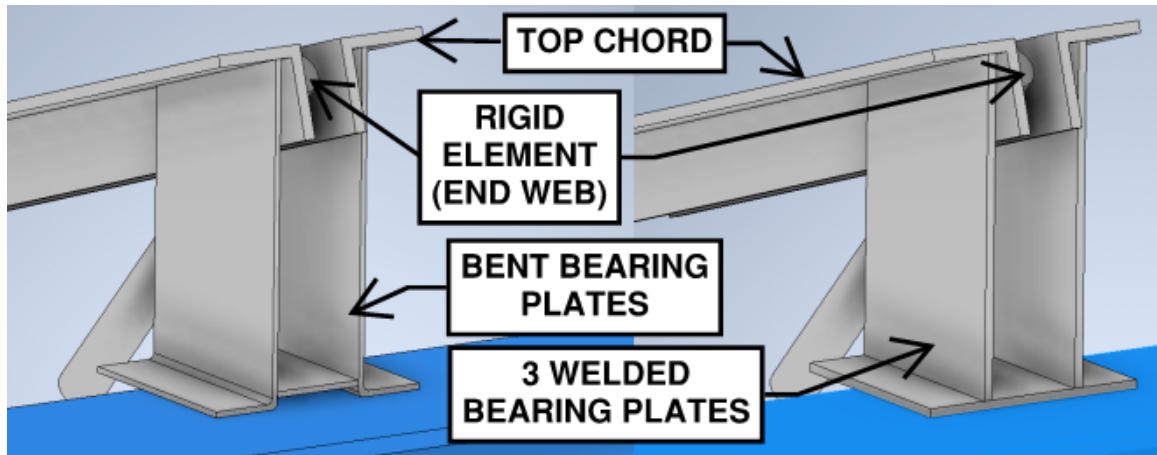


Figure 1-20 - Typical Bent Plate and 3-Plate Saddle Seats

For very high loading conditions, T-plates are typically used. T-plates are special seats prefabricated by the cut-out operation using either two plates assembled into a “T”, or two large angles placed “back to back” into a “T”, as seen in Figure 1-21. T-plates are capable of carrying much larger gravity loads than other seat configurations and are commonly used on very large and very heavily loaded joists or joist girders that use double angle end webs. However, the situations that require T-plates are for joists and joists girders so large that they are required to be fabricated one at a time, without stacking. In these conditions, it is not a significant expense to add seat stiffeners when required.

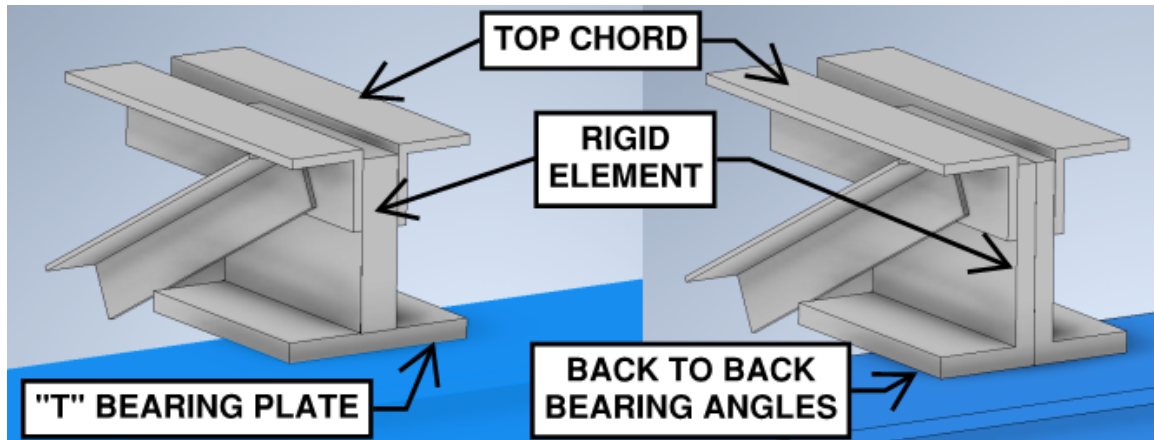


Figure 1-21 - Typical T-Plate and Back to Back Seats

1.8 Rollover Forces on Joist Seats

Now, consider the generic joist seat subjected to a rollover force “V” from the deck and carrying it to its support as seen in Figure 1-22. Due to statics, there are both horizontal reactions to resist the rollover force itself and vertical reactions forming a couple to resist the moment induced by the eccentric loading. In this condition, one side of the joist seat is in “compression”, and the other side is in “tension”, divided by the semi-rigid element. When the rollover force is directed to the right, as shown in Figure 1-22, the left side, the side opposite the direction of the force, is considered the tension side, while the right side is considered the compression side.

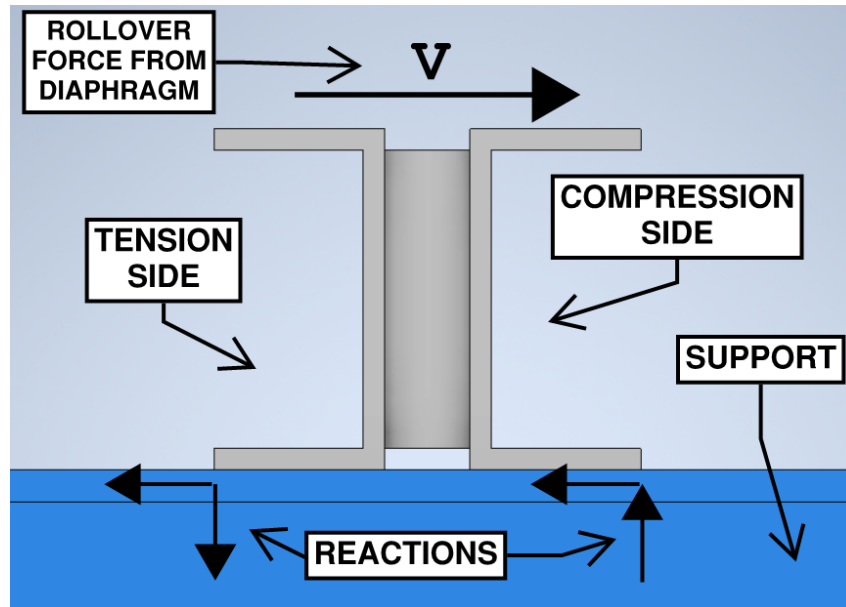


Figure 1-22 - Generic Joist Subjected to a Rollover Force

1.9 Scope and Objective

It has been identified by industry that current methods for rollover design are overly conservative and not representative of the true mechanisms present. The lack of accuracy of these methods and the subsequent lack of confidence by the joist industry has resulted in the use of alternative methods of addressing the loading, namely the use of shear collectors and seat stiffeners, ultimately leading to higher costs. The goal of this report is to further the understanding of steel joist seats subjected to rollover and to provide direction to the industry for further research to develop methods for predicting their capacities. Given that the highest relative costs for these alternatives is in smaller joists, this report will focus on the seated connections of “short span” joists, specifically the lapped seat configuration, which is the most common used in these joists.

Chapter 2 – Literature Review

2.1 Introduction

In the steel joist industry, as new code requirements for wind and other lateral considerations expanded, there was a need to develop methods for carrying those lateral loads from the diaphragm, through the joist, and to the support. In order to avoid using expensive shear collectors, these diaphragm forces needed to be carried through the joists seats as rollover forces. Over the years, there have been a number of studies that have added to and expanded the body of knowledge regarding the capacity and design of steel joist seats subjected to rollover forces. This chapter will summarize some of the major developments and outline the current methods of design used by the three largest joist manufacturers in the industry.

2.2 Resistance Based on Yield Strength – Fisher et al. (2002)

In the joist industry, the primary concern when considering the rollover strength of joist seats is the strength of the assembly at first yield, or the elastic strength, as permanent deformations of the structure are not ideal and typically considered unacceptable.

Fisher, et al. (2002) outlines resistance of Steel Joists seats subjected to rollover forces based on yield strength. This was the first method outlined for designing joist seats for rollover and it provides the basis for the majority of future research.

In this method, reactions are assumed as seen in Figure 2-1, Fisher et al. (2002), at the toes of each bearing seat angle. The rollover force is resisted by two horizontal reactions, with each being equal to half the rollover force, located at welds connecting each bearing angle to the support. Additionally, a couple also forms to resist the resulting moment with reactions in the same locations.

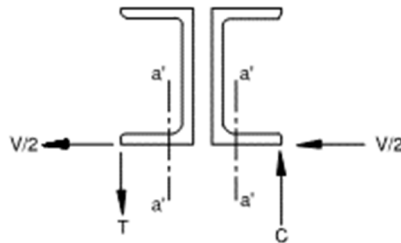


Figure 2-1 - Joist Seat Resisting Rollover Force

Yielding is assumed to occur first on the horizontal outstanding leg of the tension side bearing angle. The yielding is due to the moment created in the angle as it carries the rollover force from the top chord, or other connecting elements, to the bearing weld at the toe. This force is maximized by drawing the yield line at the edge of the k dimension, with a length assumed by drawing a 45-degree line from the edge of the weld at the toe as shown in Figure 2-2, Fisher et al. (2002). The strength of the section is based on the elastic section modulus $S = bt^2/6$. This is shown in Figure 2-2 in a top down view of the tension side angle. Note that section a'-a' corresponds to the same section a'-a' on Figure 2-1.

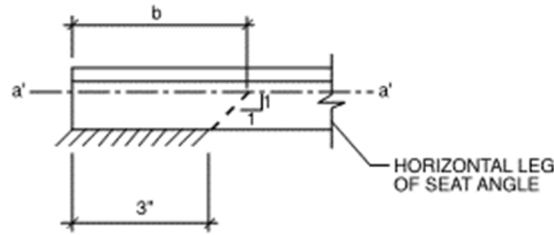


Figure 2-2 - Effective Angle Width

Using this method, the rollover capacity “V” of the bearing seat is determined by summing the moments about point *d* such that

$$V = T \frac{w_e}{h}, \quad (2-1)$$

where “T” is the maximum vertical force in the weld

$$T = \frac{M_y}{w_{leg} - k} \quad (2-2)$$

and,

w_e = bearing width (shown in Figure 1-15)

h = height of the joist seat (shown in Figure 1-15)

w_{leg} = width of the horizontal seat leg

k = section property “k” for angles seen in the AISC Steel Construction Manual

M_y = the yield moment of the seat angle: $M_y = SF_b$

$F_b = 0.75F_y$

S = elastic section modulus of the seat angle: $S = bt^2/6$

t = thickness of the joist seat

b = effective width of section in bending: $b = L_w + w_{leg} - k$

2.3 Resistance Based on Ultimate Strength – Fisher et al. (2002)

As stated before, design of steel joist seats for rollover forces is based off elastic strength. However, it is also helpful to know the ultimate capacity when considering designs under extreme loading events. It is not always plausible to use standard design methods when considering extreme loading events due to the high loading demands. As such, the much higher ultimate capacities can be utilized to prevent catastrophic failure modes. A common example is that, during an extreme wind event such as a tornado, it is preferable that a roof undergo dramatic deformations than to be sheared free from the supporting elements. The building may be damaged and require repairs, or even replacement, but it will not collapse, which keeps anyone inside the building safe. Fisher et al. (2002) outlines a method for estimating the resistances of steel joist seats for rollover forces based on ultimate strength.

At the point of failure, the joist seat is assumed to deform as shown in Figure 2-3, Fisher et al. (2002), below. In this state, the rollover force is resisted by an equal but opposite horizontal reaction by the tension side weld at the toe of the bearing angle and the couple that forms to resist the resulting moment with a negative reaction at the same location and a positive reaction some distance within the profile of the seat angle on the compression side, assumed conservatively to be at the heel of the compression side seat angle.

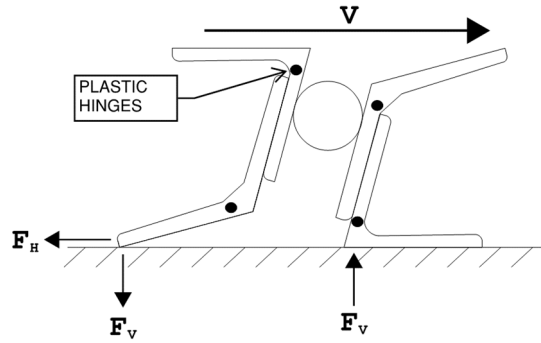


Figure 2-3 - Seat Failure Mode

The two failure modes are rupture of the tension side bearing weld, or the shear failure of the vertical leg of the tension side bearing seat angle, just below the rigid element. The tension side bearing weld will typically be the ultimate failure element in all standard configurations. The design loading on this element, “ F_a ”, is the principle stress resulting from combining the horizontal reaction and negative component of the couple acting on this weld, expressed as

$$F_a = \sqrt{F_H^2 + F_V^2}, \quad (2-3)$$

where

F_H = vertical component of the reaction, in terms of “ V ”, $F_H = V$

F_V = horizontal component of the reaction, in terms of “ V ”, $F_V = V \cdot H/m$

V = magnitude of the lateral rollover force applied to the joist seat

h = height of the bearing seat as previously depicted

m = length of the moment arm of the reaction couple as previously depicted

The ultimate capacity “ R ” of the weld is determined by von Mises yield criteria and is equal to

$$R = \left(\frac{F_{exx}}{\sqrt{3}} \right) (t_w)(\sqrt{2})(L_w), \quad (2-4)$$

where

F_{exx} = is the yield strength of the weld material

t_w = fillet size of the weld

L_w = length of the bearing weld

Setting “ F_a ” equal to “ R ” and solving for “ V ” yields

$$V = \frac{\left(\frac{F_{exx}}{\sqrt{3}} \right) (t)(\sqrt{2})(L_w)}{\sqrt{1 + \frac{H^2}{m^2}}}. \quad (2-5)$$

2.4 Determining Strength Through Testing

Fisher et al. (2002) points out that many assumptions relative to the internal strength of joist seat assemblies are beyond the control of the building designer, and their strengths cannot be easily calculated. Instead, the authors believed the allowable lateral force capacity for any given joist seat can be based upon the ultimate strength procedure. They indicate the best way to estimate the internal strength of a joist seat is through experimental testing and present some results from experiments performed by Vulcraft.

The Vulcraft testing included a field of 10 tests from “H-series” joists, an older series of joists similar in scope to current “K-series” joists. The Joists used were 8H3, 24H6, and 26H8 joists. The seated connections of these series of joists would have used the lightest bearing seat angles in the industry at the time with thicknesses of 0.109 in, 0.145 in, and 0.163 in, respectively, assembled in a butted seat configuration.

The test setup is shown in Figure 2-4, Fisher et al. (2002), and constituted welding the joist seats to a rigged support, applying the design vertical loading, and then applying a lateral rollover force until failure. The rollover force was applied through a rigid plate welded to the top chord angles of the seat assembly. It should be noted that the weld connecting the seat assembly to the rigid support was four inches and was sized equal to the angle thickness. Today, the Steel Joist Institute specifications only require two, one-eighth inch fillet welds that measure two and a half inches long.

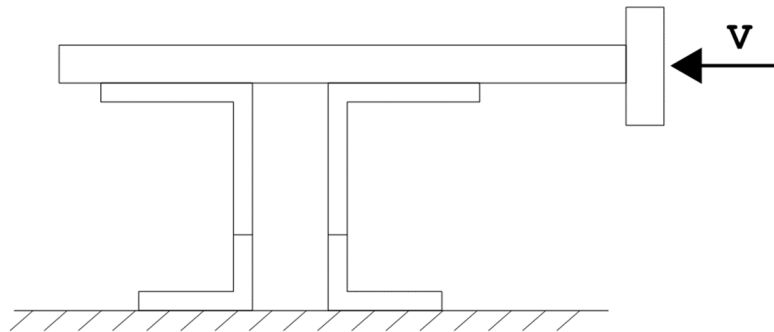


Figure 2-4 - Load Arrangement for Vulcraft Testing

The failure modes of all of the 8H3's and 24H6's was rupture of the weld connecting the joist's seat to the rigid support on the tension side. The 26H8 tests were ended due to loading constraints of the test apparatus. There was no failure of internal seat welds during any of the tests. However, it is important to note the weld failure only occurred after the formation of significant lateral distortions.

Fisher et al. (2002) notes it is interesting to compare the average failure loads from these Vulcraft tests to the estimated capacities of the seats by the ultimate strength design method, indicating that such a comparison would seem to show a reasonable correlation.

The authors indicate, as can be seen from the deformed shape, that the seat assembly would undergo significant lateral deformations at the ultimate load. As previously mentioned in this section, it is not preferable to have plastic deformations, or even large elastic deformations, in any part of the structure. The authors indicate that it is suggested by the industry to limit deformations of this nature, pertaining to shear collectors between the diaphragm and supporting elements at large, to 0.25 inches. However, they point out that even with this limit, there would still be some yielding in the connection.

Based on this recommendation, resistance based on ultimate strength is a widely accepted method of design. However, given the difficulty of determining the lateral deflections for the near infinite combinations of joist seats, the three major joist manufacturers in the industry choose to utilize the elastic method for designing joist seats for rollover forces. The issue with the elastic method is that, when compared to the experimental data, it is very conservative. As a result of such a conservative approach, the predicted strength of the joist seats is inadequate for many design requirements. Therefore, seat stiffeners or other alternate design methods must be pursued. Additionally, it is noted that none of the methods previously mentioned may be accurately applied to more unique seat configurations such as “saddle seats” or “T-plates”.

2.5 Behavior of Open Web Steel Joist Seats Subjected to Lateral Loads

Realizing the aforementioned design methods were overly conservative and potentially not applicable to all joist seat configurations, Doyle (2010) conducted additional research to investigate further.

Doyle (2010) conducted 81 different tests of twenty-seven common joist configurations and loaded them to failure. Seat configurations included standard “Lapped” seats, prefabricated “Lapped-in” seats, “Pegged” seats, “3-Plate Saddle” seats, and “T-Plate” seats. This was backed up by finite element models of the same configurations.

What set Doyle (2010) apart from previous research was the configuration of his test setup. Most previously conducted tests by other researchers used a single seat that is forced over by a loading element. Doyle (2010) points out that this does not properly capture the failure mechanism of joist seats under rollover, as it allows the joist seat to cant over relative to the base as shown in Figure 2-5. In reality, attachment to the continuous deck sheets, deck edge angles, cell closures and other fairly rigid elements, will cause what better resembles a racking motion, as was depicted by Fisher et al. (2002) and shown again in Figure 2-6.

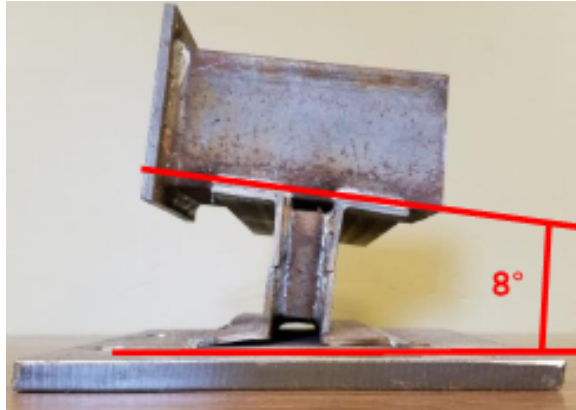


Figure 2-5 - Canting Joist Seat

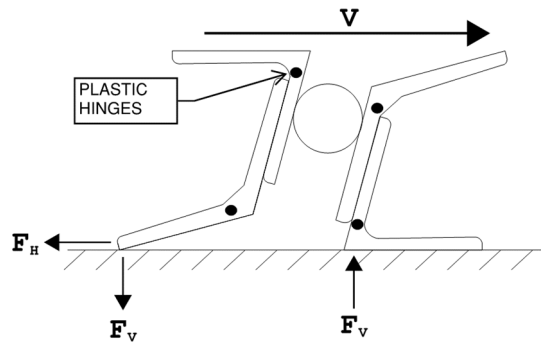


Figure 2-6 - Racking Joist Seat

This is also shown to be the case in the field where rollover and uplift have resulted in deformations of joist seats. At the time of this report, there is only one case known by the Steel Joist Institute where such a failure has occurred. Typically, in a high load wind scenario, the deck is pulled from the joists, or the bearing element is pulled from the support, before a rollover failure results in the joist being pulled from the bearing element. The single case can be seen in Figure 2-7. Despite the large deformations in the bearing angle of the joist seat, the top chord angles exhibited a near perfect racking motion, with essentially no cant.



Figure 2-7 - Field Examples of a Rollover Failure

Doyle (2010) simulated a more realistic testing scenario by loading two joist seats connected by a rigid element, similar as shown in Figure 2-8. The joist seats are then loaded simultaneously. As they begin to deflect, the rigid element connecting them will force a racking motion more similar to the real world loading scenario.

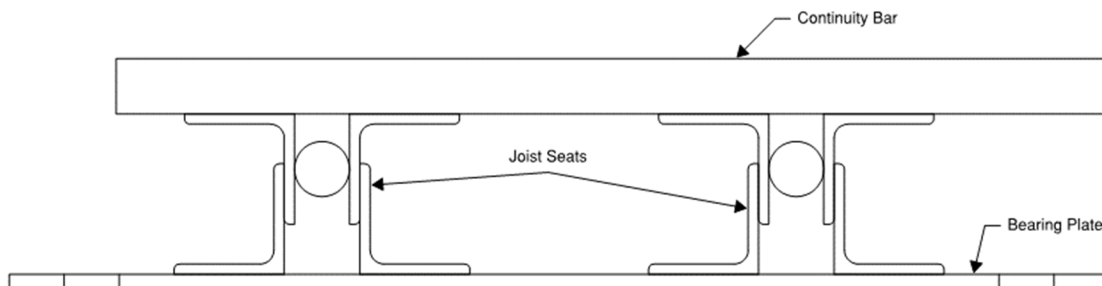


Figure 2-8 - Test Setup With Two Joist Seats Connected by a Rigid Element and Loaded Simultaneously.

The joist seat specimens were fabricated by CMC Joists in accordance with their quality control practice and then shipped to Villanova for testing. However, it should be noted that the weld connecting the toe of the bearing angles to the bearing plate, the bearing weld, was four inches for K series joist seats and six inches for LH series joist seats. This deviates from the standard bearing weld length as indicated by SJI (2015)

which is shown below in Table 2-1. This is relevant to note as the length of the bearing weld has a large impact on the elastic and ultimate strength of the joist seat.

Table 2-1 - Minimum Bearing Weld Lengths

JOIST SECTION NUMBER ¹	MINIMUM FILLET WELD	MINIMUM BEARING SEAT BOLTS FOR ERECTION
K1-12	2– 1/8" x 2 1/2" (3 x 64 mm)	2– 1/2" (13 mm) A307
LH02-06	2– 3/16" x 2 1/2" (5 x 64 mm)	
LH07-17, DLH10-17, JG	2– 1/4" x 2 1/2" (6 x 64 mm)	2– 3/4" (19 mm) A307
DLH18-25, JG ²	2– 1/4" x 4" (6 x 102 mm)	2– 3/4" (19 mm) A325
⁽¹⁾ Last digit(s) of joist designation shown in load table.		
⁽²⁾ Joist Girders with a self weight greater than 50 plf (0.73 kN/m).		

2.5.1 Doyle (2010) Findings

Lapped and pre-assembled lapped-in seats were the most consistent and noted the importance of connecting welds being the full length of the seat material in order to prevent torsional effects throughout. This is important to point out again because the typical weld specified by SJI is smaller than the length of the joist seat, so there are likely to be torsional considerations in the typical configuration. Ultimately, Doyle (2010) indicated that both the elastic strength method and ultimate strength method were conservative and could be used for design.

Pegged seats, although similar to lapped seats in many aspects, have additional considerations due to the configuration of the peg. Unlike the lapped seat, which uses the long welded lap that distributes the load across a long portion of the bearing angle, the peg seat concentrates forces within a single area of the bearing seats. This can make internal welds and the vertical leg of the bearing angles the critical design elements.

Doyle (2010) notes that compared to lapped configurations, pegged seats had larger rotations and total deflections. This is likely an indication of additional yielding in the vertical leg of the bearing angles.

For T-Plates and 3-Plate Saddles, Doyle (2010) indicated that neither the Elastic Strength Method or the Ultimate Strength Method are applicable. Unlike the other standard configurations which have homogeneous bearing angles, these seat configurations use vertical plates connected to horizontal bearing plates with fillet welds which must be able to fully transfer the loading from the vertical elements to the horizontal bearing elements. Due to the compact spacing of these welds, the couple forces that form to prevent overturning of the vertical elements are very large, which typically makes the fillet welds connecting the vertical and horizontal elements the critical design parameter. However, even when the welds are sized appropriately, these forces cause significant local bending in the horizontal bearing plate, which is typically much thinner than the vertical plate.

As was previously indicated, existing methods for estimating the capacity of steel joist seats subjected to rollover forces are not applicable to these seat configurations. Instead of adapting these methods, Doyle (2010) used finite element models to match experimental results. Using two dimensional frame elements, Doyle (2010) recreated the seat's configurations and found reasonable matches to model performance and experimental performance of the joist seats.

2.6 Green and Sputo (2002) Yield Line Theory

Green and Sputo (2002) discusses and derives a model to predict the capacity of joist seats subjected to uplift forces. When subjected to uplift forces, joist seats have a tendency to form yield lines about the welds that connect the bearing angles to the support. By simplifying the geometry of the yield line, as can be seen in Figure 2-9, Green and Sputo (2002), and applying the virtual work method, the allowable uplift force can be obtained as

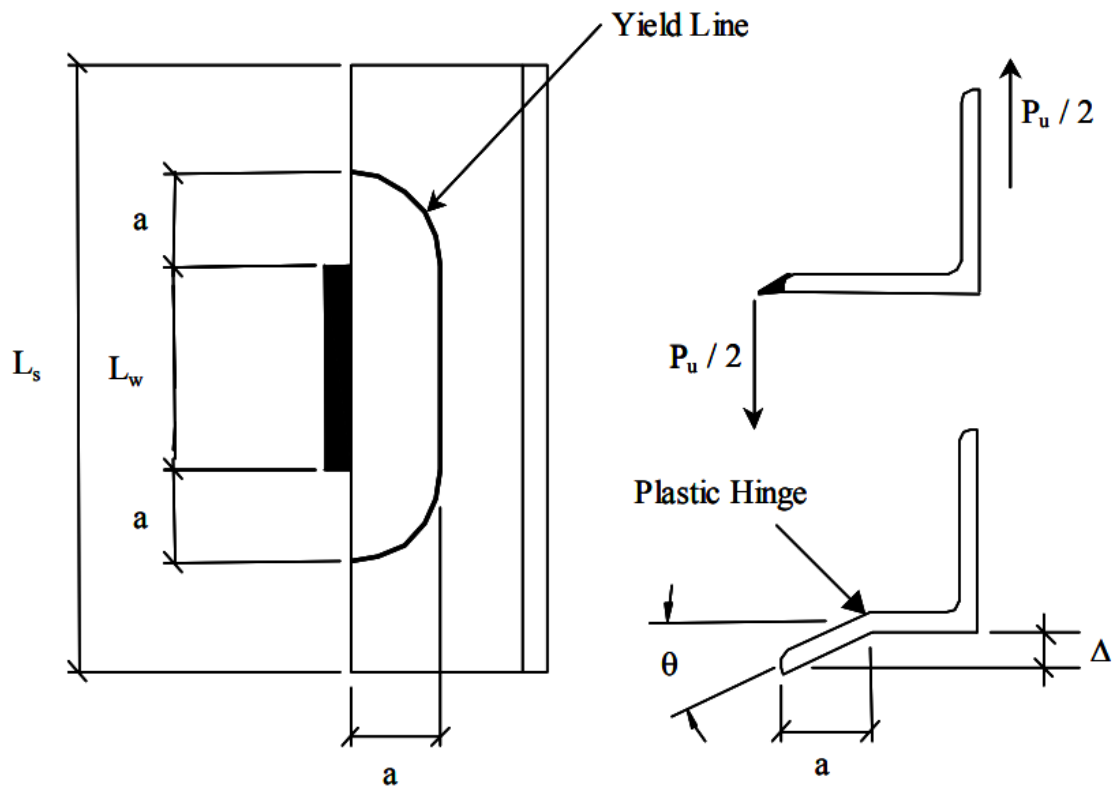


Figure 2-9 - Simplified Yield Line of Bearing Angles Subjected to Uplift Forces

$$P_u = \frac{2M_p L_{YL}}{a}, \quad (2-6)$$

where

M_p = plastic moment capacity of the plate, per unit length of plate = $F_y Z$

- L_{YL} = length of the yield line, the lesser of $(L_w + \pi a)$ and L_s
- L_w = length of anchorage weld
- L_s = length of the seat angle
- F_y = average 0.2% offset yield stress of the steel angle
- Z = plastic section modulus of unit length of plate which is $t^2 / 4$
- t = thickness of seat angle leg

Then the experimental test data can be analyzed to find the best fit for the distance “a”.

Green and Sputo (2002) found this number to be equal to $2.3t$.

2.7 Applying the Green and Sputo (2002) Yield Line Theory

Seeing the relationship between the behavior of joist seats under uplift and the tension side of a joist seat subjected to rollover, the Alabama division of Vulcraft Joists theorized a model which used the yield line theory from Green and Sputo (2002). The result was a yield line forming on the tension side of the joist seat, and an idealized positive reaction forming on the compression side of the joist seat as shown in Figure 2-10. The left diagram shows a top down view of the bearing angles with the idealized formation of a yield line. The right diagram shows section view of the same seat with the static reactions due to the rollover force. The distance between the negative reaction in the tension side support weld and the idealized positive reaction on the compression side is called “m”. The magnitude of these reactions can then be found by summing the moments about the support weld on the tension side. The maximum

allowable rollover force on a joist seat can be found by similarly applying this concept to the Green and Sposito (2002) yield line equation such that

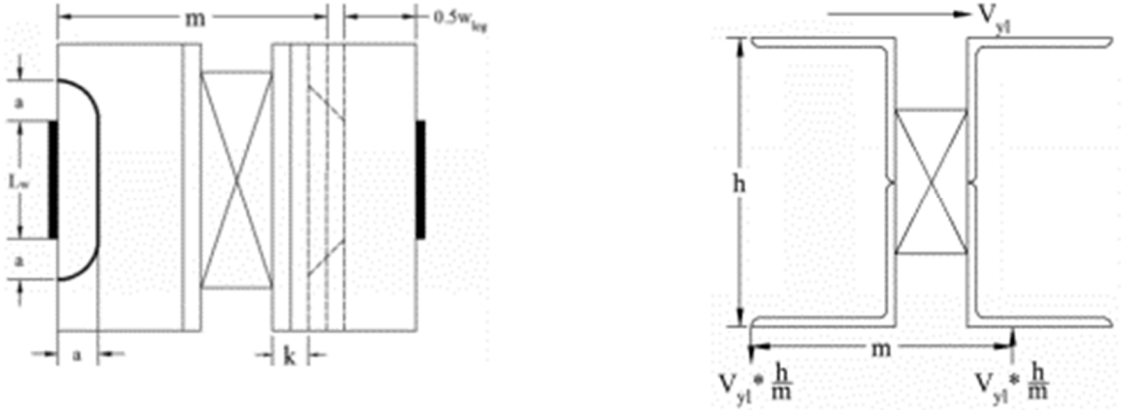


Figure 2-10 - Applying the Yield Line Theory from Green and Sposito (2002) to Joist Seats Subjected to Rollover Forces

$$P_u = \frac{M_p L_{YL}}{a} \quad (2-7)$$

becomes

$$V_{yl} = \frac{M_p L_{YL}}{a} * \frac{m}{h}, \quad (2-8)$$

where

- V_{yl} = magnitude of the lateral rollover force applied to the joist seat based
- H = height of the bearing seat as previously depicted
- m = length of the moment arm of the reaction couple as previously depicted
- M_p = plastic moment capacity of the plate, per unit length of plate = $F_y Z$
- L_{YL} = length of the yield line, the lesser of $(L_w + \pi a)$ and L_s
- L_w = length of anchorage weld
- L_s = length of the seat angle
- F_y = average 0.2% offset yield stress of the steel angle
- Z = plastic section modulus of unit length of plate which is $t^2 / 4$

t = thickness of seat angle leg.

This method would appear to be most applicable compared to other methods when realizing the typical manner in which joist seats are connected to supports in the field. As previously noted, past research has been conducted with anchorage weld lengths longer than required by SJI, often even the full length of the joist seat. When shorter weld lengths are used, it is likely that this yield profile can be expected.

2.8 Internal Stiffness vs. Bearing Seat Capacity

Lapped seat configurations are the most common on K series joists, representing 70%-80% of seats used. This is primarily due to simplicity during fabrication and the ease with which they can be assembled.

Lapped seats can be assembled with two different configurations of welds. The first configuration uses two welds located on the inside of the seat, while the second configuration uses four welds located on both the inside and outside of the seats, as can be seen in Figure 2-11. The two weld configuration is easier to fabricate. However, it would seem that using the four weld configuration would provide additional strength to the joist seat when subjected to rollover forces. To investigate the benefit of using the four weld configuration, the Steel Joists Institute funded research at Bucknell University to use computer simulations of the two configurations to see what behavior can be observed and the differences in strength. The exact results of the tests can be seen in Figure 2-12, Abreu, Ziemian (2017). The results can be summarized as a 15% increase in

strength for seats made out of thicker material (0.25 in.) and up to a 22% increase in strength for seats made out of thinner material (0.155 in.).

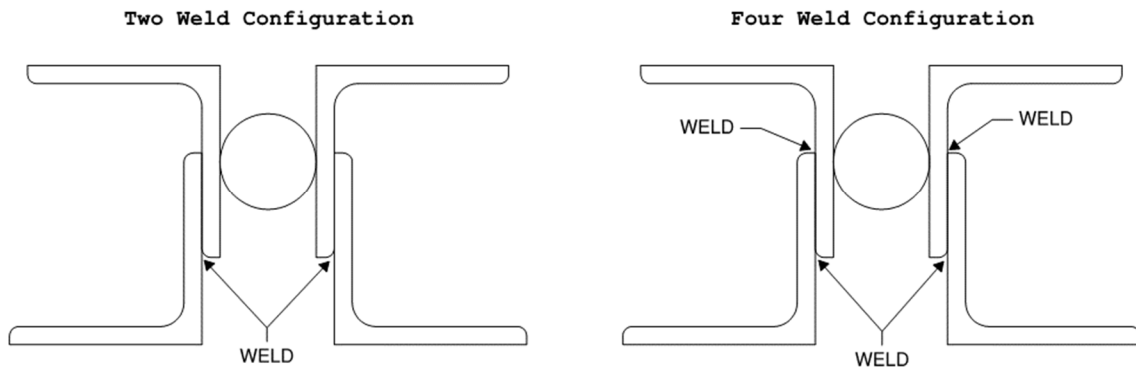


Figure 2-11 - Two Weld vs. Four Weld Lapped Configuration

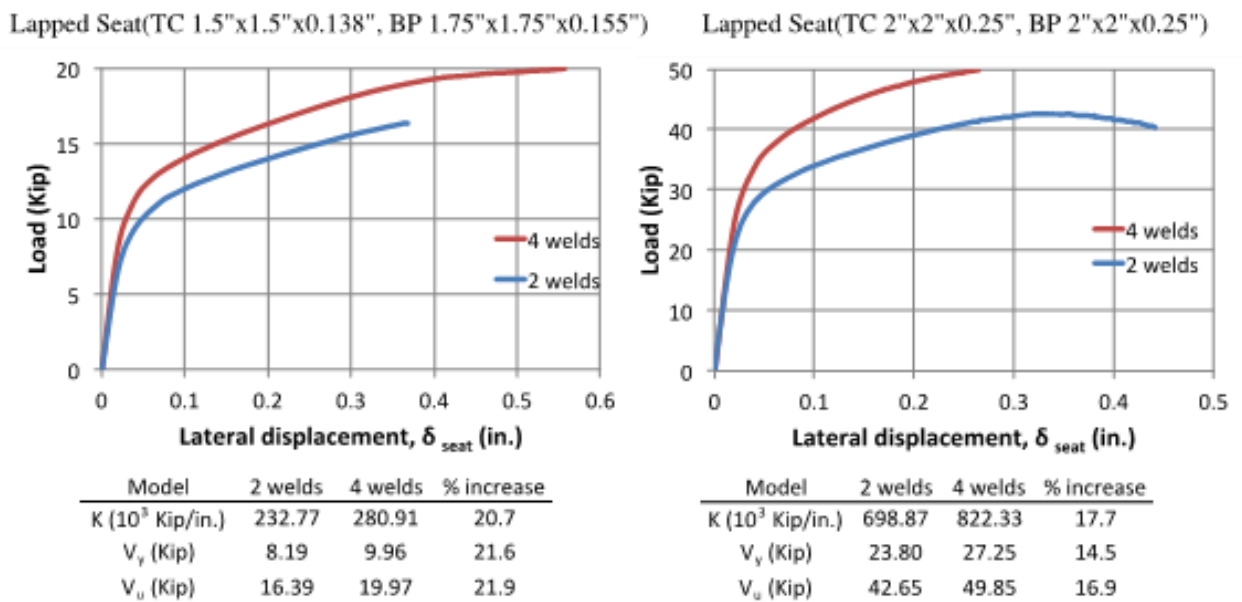


Figure 2-12 - Performance of "2-Weld" vs. "4-Weld" Configurations Subjected to Rollover

The only difference between these configurations was the location and number of welds. While the four weld configurations had higher rollover capacities, the failure modes of all configurations were the same. Notice in the loading curves that the four weld configuration exhibits slightly higher stiffness with a higher ceiling in both the

elastic and inelastic regions. It would seem that the additional welds on the four weld configuration increased the stiffness of the assembly which resulted in a larger moment arm in the couple force resisting the rollover, which in turn means smaller couple reactions that the seat angles are required to resist.

It is easy to picture how the positive reaction of the couple force could be moved further out along the horizontal leg of the compression side bearing angle by using the four weld configurations when compared to the two weld configurations when looking at the deformed shapes of each, as seen in the models performed by Abreu, Zeimian (2017) in Figure 2-13. The additional welds of the four weld configuration keep the toes of the bearing angles restrained to the top chord, which is braced against rotations.

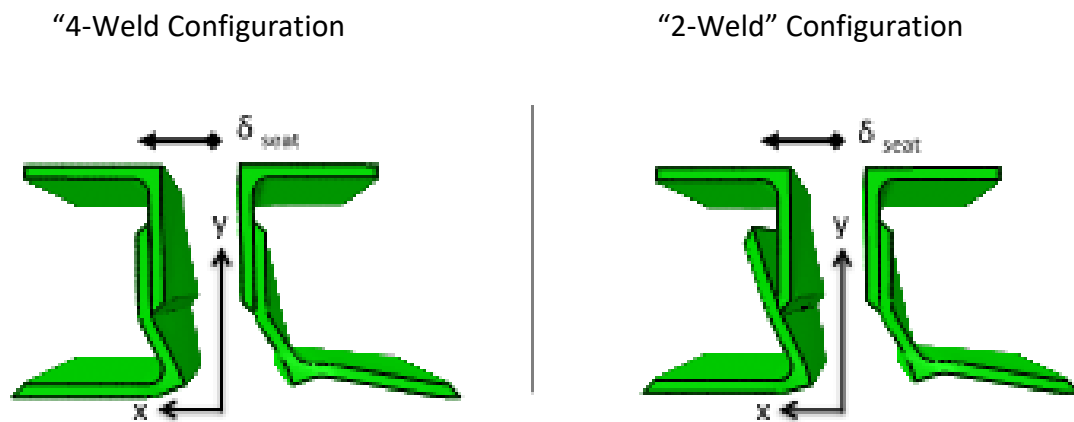


Figure 2-13 - Deflection Assemblies of "2-Weld" and "4-Weld" Configurations

It is important to notice that in all the methods that have been presented, the assumption of the length of the moment arm, m , varies widely. This is not a small matter, as it can be seen that the length of this moment arm can have a significant effect on the magnitude of the couple forces, and thus the capacity of joist seat

subjected to rollover. Statics allow for certainty that the negative reaction is in the anchorage weld on the tension side of the joist seat. However, the complexity of the seat configurations means that it is very difficult to estimate the location of the positive reaction.

If the configuration was infinitely rigid, the positive reaction would be in the toe of the angle compression side bearing angle. If it were infinitely flexible, the positive reaction would be very near the heel. This is the conservative assumption, but for industry applications, it may be considered too conservative. All seat configurations do have some rigidity, and increasing that rigidity can produce very real increases in rollover capacity. It would be productive to develop a method that balances conservative design and reality, and the length of m will be critical in doing so.

2.9 Summary

There are many existing methods for designing steel joists for rollover forces. The ultimate methods are relatively accurate, while the elastic methods are very conservative and are not representative of the actual failure mechanism of the joist seat. Given that industry predominately designs for elastic responses, these conservative design methods are not economical and often lead to stiffeners in the joist seat which are very expensive for both fabrication and shipping. Therefore, it would be beneficial to develop a new method for assessing the capacity of joist seats subjected to rollover that would more accurately predict the failure mechanism.

Chapter 3 – Methods

3.1 Introduction

As indicated in the background section of this report, it would be beneficial to more accurately predict the capacity of steel joist bearing seats subjected to rollover forces. It would appear, based on theories and research conducted by the Alabama division of Vulcraft Joists, that applying yield line theory similar to Green and Sposito (2002) as a model for the tension side of a steel joist seat under rollover could be an accurate method of estimating capacity, and may better reflect the actual failure mechanism. In order to verify this, a new field of tests needs to be conducted using parameters, like bearing weld lengths and weld locations, that more accurately reflect field conditions. This chapter will outline the details for these parameters and the overall test setup used in the experiments conducted during this work.

3.2 Test Setup

The test setup is divided into two areas: the testing table and the test specimen. The test specimens, shown in Figure 3-1, consisted of two identical joist seats, welded per the standard Steel Joist Institute requirements to a 0.25 in. plate and 1.5 in. continuity bar used to apply the load. All test specimens were fabricated at the Texas division of Vulcraft joists according to their quality assurance standards and the standards of the Steel Joist Institute.

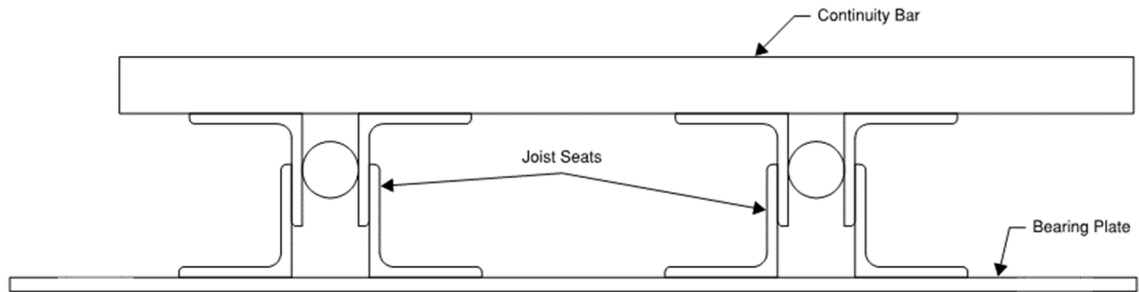


Figure 3-1 - Test Specimen

The test table can be seen in Figure 3-2 and consists of five main parts: a frame, a specimen platform, a hydraulic ram, a load transfer frame, and a pair of bearing seat stiffeners. Note that bolts are removed from the model for clarity.

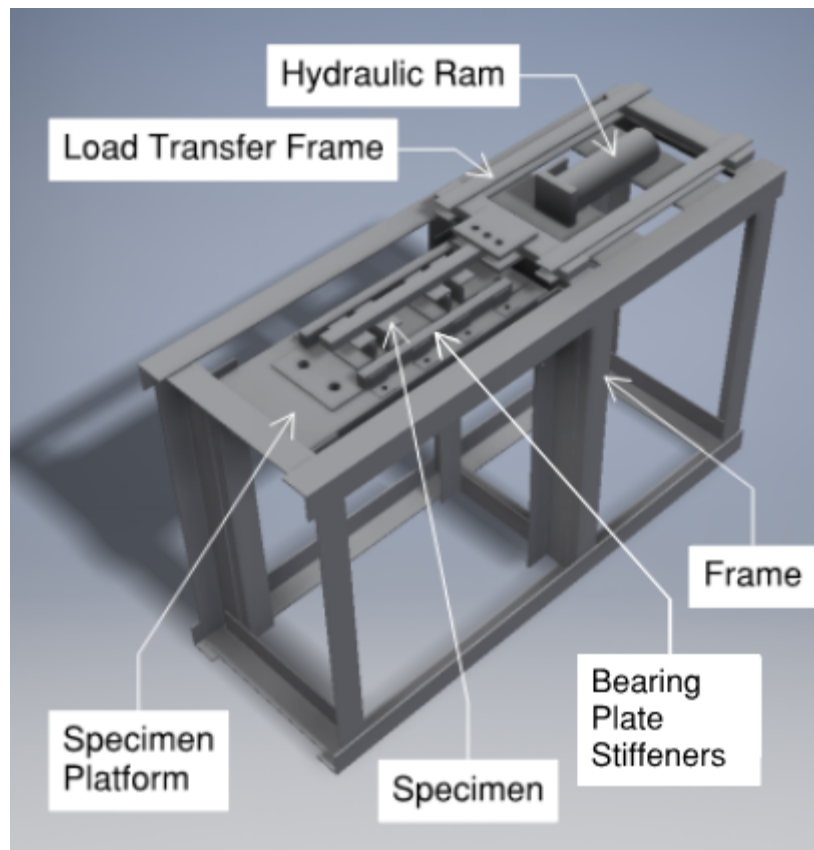


Figure 3-2 - The Test Table Used to Conduct the Experiments Shown Loaded with a Specimen

The frame is the primary assembly that holds all of the other components in place. The frame contains several stiffened elements to reinforce the load path to the joist seats. The frame and other components of the table were constructed by a number of contributors from the Quality Assurance and Production teams from the Texas division of Vulcraft Joists.

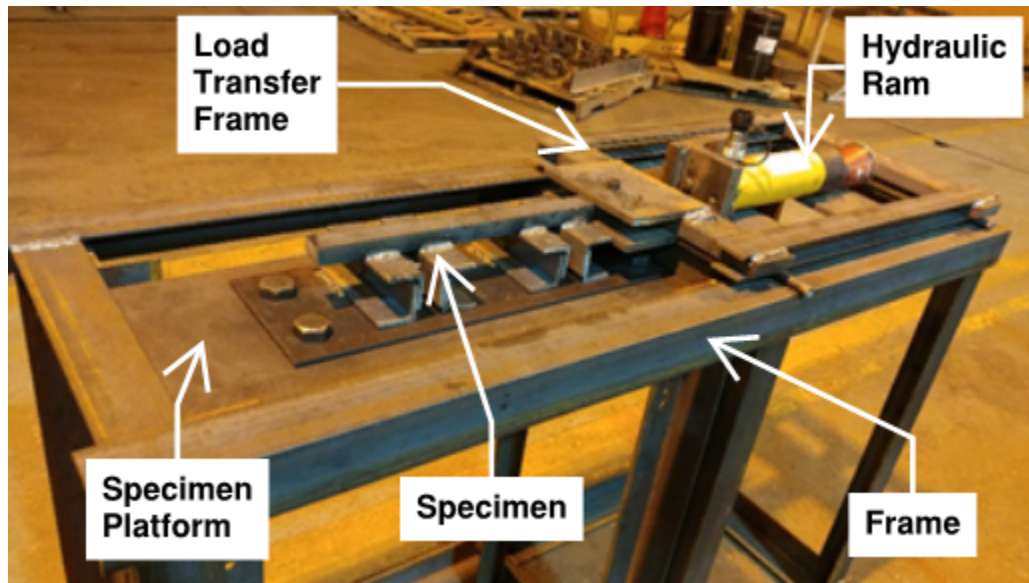


Figure 3-3 - Test Frame Shown Holding the Other Elements Before Installing Stiffeners

The specimen platform, shown in Figure 3-4, is a large, rigid 1 in. thick plate that the specimens are attached to via four, 1 in. bolts. The platform has the ability to be adjusted up or down to accommodate different joist seat depths as required. This is accomplished using a bolted connection and a series of holes located on the reinforced legs of the testing table frame. Load path was particularly important in this part of the test setup. It was not desirable for the forces to be transferred through the bolted connection that allowed the specimen table to be raised and lowered, as doing so would introduce a number of “kinked” connections for the load path. Therefore, the specimen

table was butted up against a stiffened angle with a transfer plate connected directly to the hydraulic ram. The specimen platform was sized to allow room for the string potentiometer used to measure deflections.

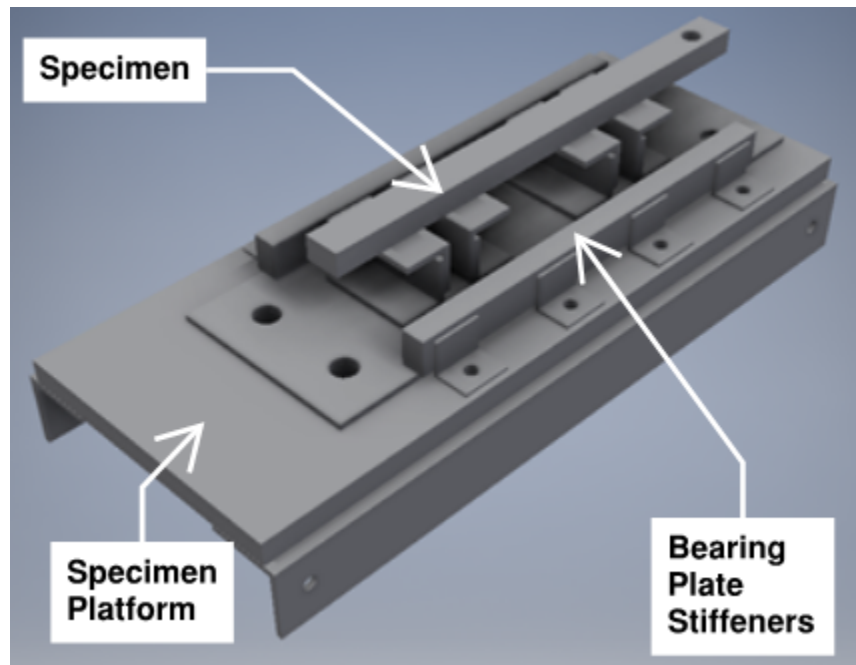


Figure 3-4 - Specimen Platform Shown Loaded With a Specimen and the Bearing Plate Stiffeners Attached

A hydraulic ram was used to load the specimens. Pressure was applied to the hydraulic ram using a manual hand pump. The hydraulic ram was bolted to a stiffened housing that allowed it to be removed when needed. In initial testing, it was found that the connection between the ram and the plate was not stiff enough, and the hydraulic ram had a tendency to rise as depicted in Figure 3-5. To prevent this, a U-bolt was added to restrain uplift of the hydraulic ram.



Figure 3-5 - Hydraulic Ram Uplift Before Modification of the Test Setup

The load transfer frame, shown in Figure 3-6, is a free-floating frame that carries the loading from the hydraulic ram to the specimen. This frame allows the rollover force to be applied in tension rather than compression, which combined with the frame's free float nature, helps to keep loading along the desired vector and reduces any additional induced moments in the specimens due to small misalignments of the test setup. To keep the load transfer frame at the appropriate elevation, and minimize any friction with the frame, it was set on lubricated rollers that allowed it to translate back and forth as the test was conducted with negligible friction.

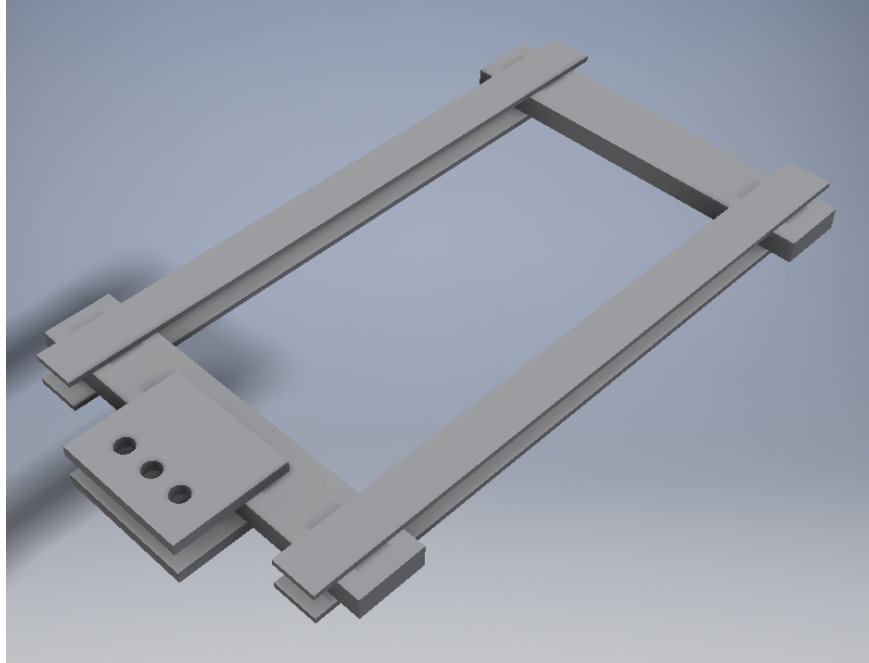


Figure 3-6 - Load Transfer Frame Used to Carry Load from the Hydraulic Ram to the Specimen

The final parts of the testing table were the bearing plate stiffeners. In preliminary testing, the specimens, were anchored to the specimen platform by only four bolts located near the corners. With this configuration there was substantial warping in the bearing plates. This is easily visible due to the formation of a gap, shown in Figure 3-7, between the bearing plate and the specimen platform. This gap does not occur in practice because real world bearing conditions would either be a 1 in. embedded plate, or the top chord of a joist girder, which, due to a number of code requirements, would have a minimum size of 2L 2½ x 2½ x .188. To account for the larger stiffness of the real word bearing condition two stiffener bars were added that could be used to restrain the bearing plate as shown in Figure 3-7. Further testing showed that this reduced the warping of the specimen bearing plates to negligible levels.

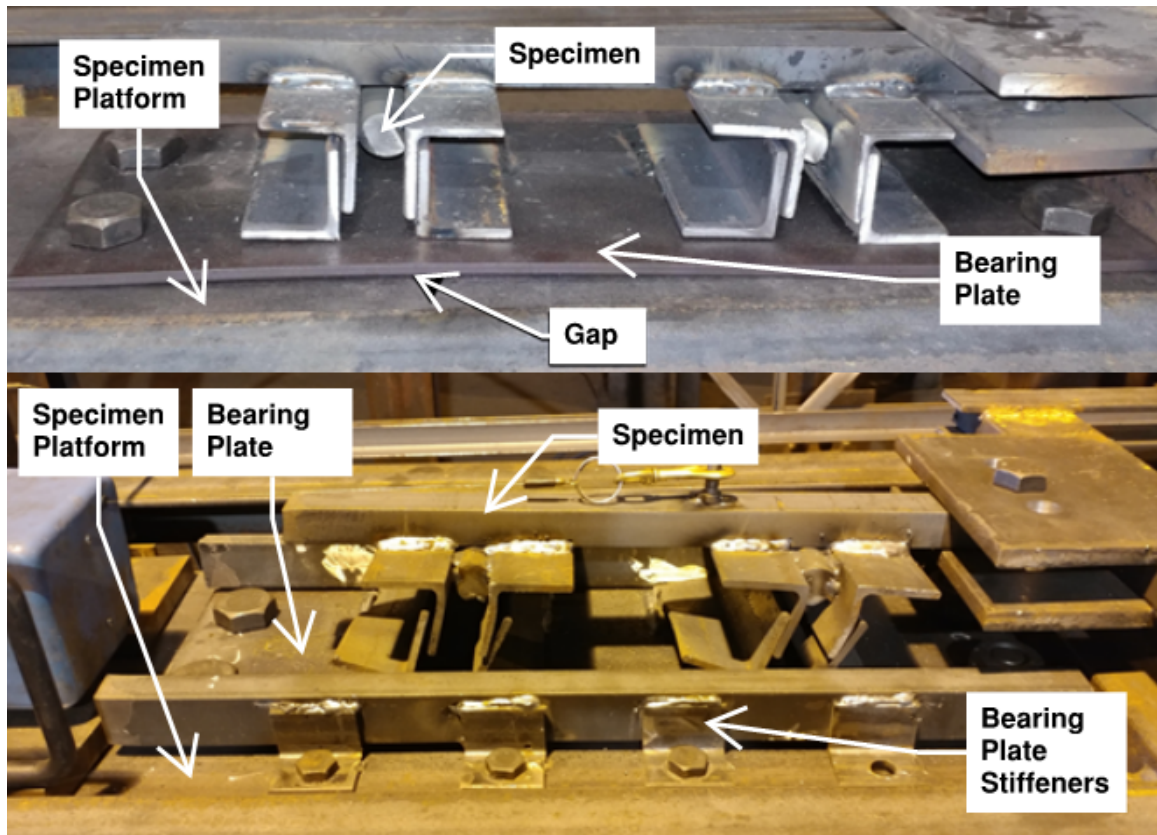


Figure 3-7 - Added Stiffener Bars Preventing Warping of Bearing Plate

3.3 Instrumentation

An in-line load cell, shown in Figure 3-8, was used to record loading. A string potentiometer was used to measure displacements. Collecting the displacement was more difficult, as connecting anywhere directly to the frame would subject the data to a number of deformations throughout the frame that would be impossible to quantify or fully prevent. This was addressed by placing the linear transducer on the specimen plate with the specimen and connecting it directly to the specimen's continuity bar as shown in Figure 3-9. As a result, additional deformations in the frame or between other components would not have any impact on the measured deflection of the specimen. The yield point of the specimen assembly was estimated by identifying the end of the

linear region of load displacement curves generated from these instruments during testing.

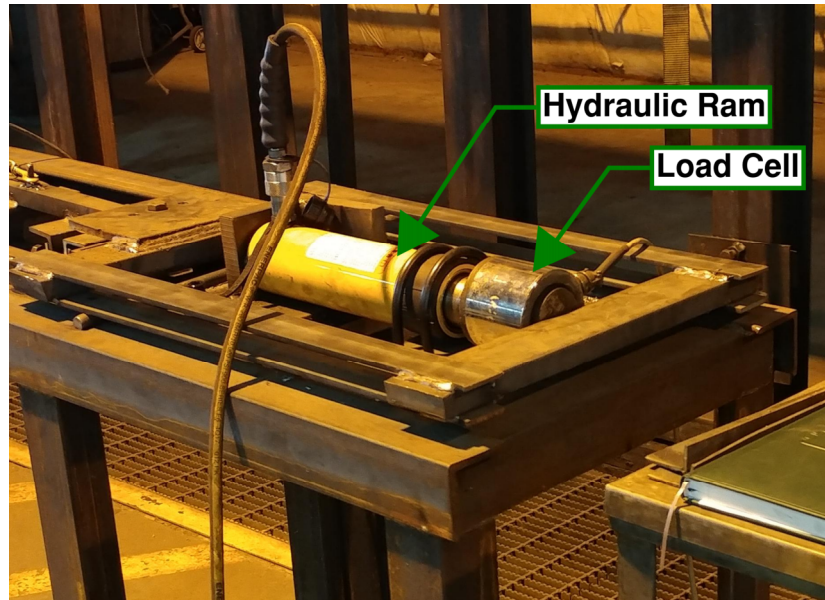


Figure 3-8 - Load Cell Located Between the Hydraulic Ram and the Load Transfer Frame

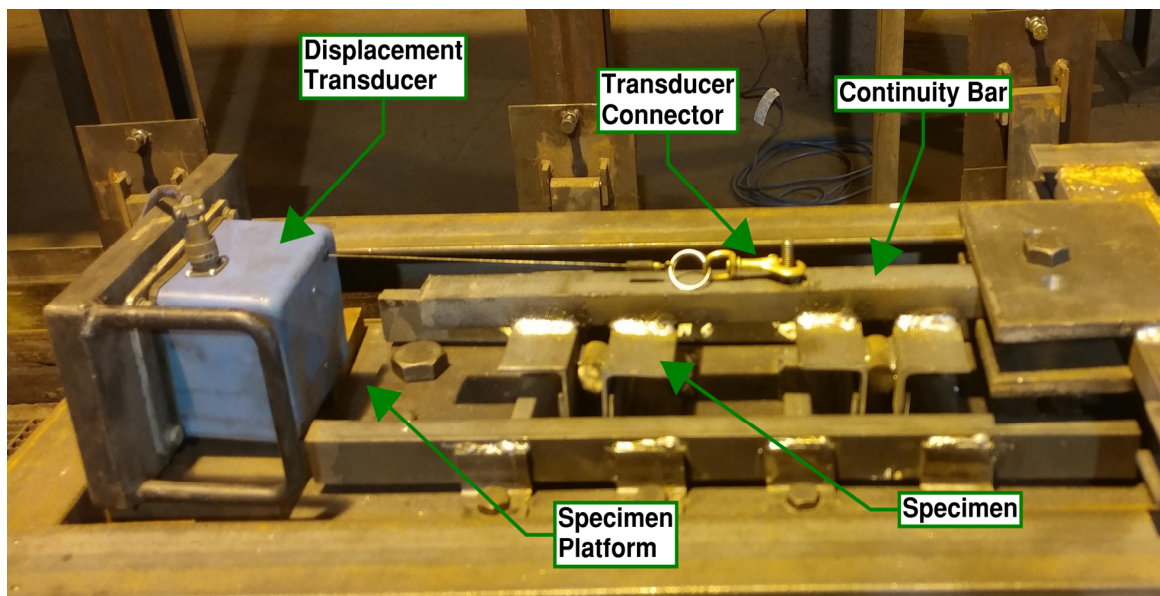


Figure 3-9 – String Potentiometer on the Specimen Platform

3.4 Data Acquisition System

The data acquisition system used in these test was originally designed to collect total load and mid-span deflection data for full scale open web steel joist tests paired with a closed loop pneumatic and hydraulic loading system. The system software was initially designed to collect only a few data points at predetermined loads or displacements. The system was adapted for the tests discussed in this report to collect data continuously.

3.5 Specimen Details

Fifteen joist seat pairs in five different configurations were tested. All of the joist seat pairs were in the lapped seat configuration, shown in Figure 3-10, which is the most common in the steel joist industry. The lapped seats were welded with the “Two Weld” configuration, meaning that weld was only added connecting the toe of the vertical leg of the bottom chord to the vertical leg of the bearing angles. This is sometimes referred to as the inside weld. This is the standard weld configuration in industry, and as such, the industry standard weld length of four inches was used. The only other internal weld in the seat assembly is the “safety weld,” which is applied at the interface between the vertical legs of the top chord and bearing angles. This weld is added for shipping purposes but was found to impact the joist seat’s response to rollover forces.

The properties of each specimen are shown in Table 3-1. These values shown are the measured properties, not the idealized properties. The five-digit specimen designations represent the properties of the bearing angles used in the specimens. The first two digits correlate to the angle size, and the last three correlate to the angle thickness. For

example, a L 2 in. x 2 in. x 0.188 in. would have a designation of 20188. The final letter in the designation correlates to the multiples of each specimen.

It is important to notice the location of the bearing weld, labeled " L_w " in Figure 3-10. Governing codes do not provide any requirements for the location of the bearing weld on the joist seat. It was assumed the worst case scenario would be with the bearing weld located at the end of the seat. This location would produce the shortest yield line and also produces additional torsional effects.

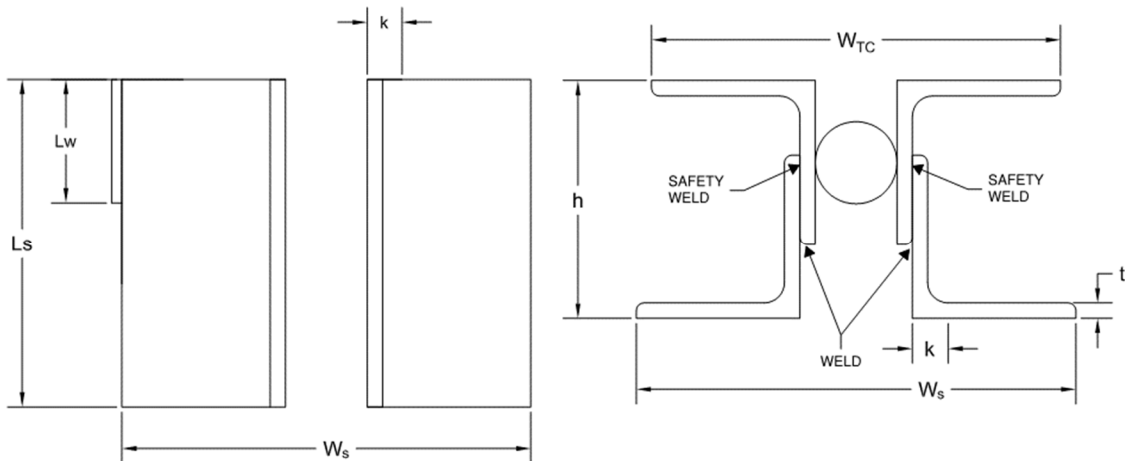


Figure 3-10 - Standard Lapped Seat Configuration

Table 3-1 - Properties of the Specimens to be Tested

Specimen Designation	h (in)	Angle Size (in)	t (in)	ws (in)	WTC (in)	Fy (ksi)	Lw (in)
20250-A	3	2x2	0.250	5.500	5	58	2.500
20250-B							2.500
20250-C							2.500
20188-A			0.188	5.376		57	2.625
20188-B							2.500
20188-C							2.500
20163-A			0.155	5.310			2.375
20163-B							2.375
20163-C							2.250
15155-A	2.31	1.5x1.5	0.155	4.310	4		2.500
15155-B							2.500
15155-C							2.500
15133-A	2.226		0.113	4.226		2.500	
15133-B						2.500	
15133-C						2.375	

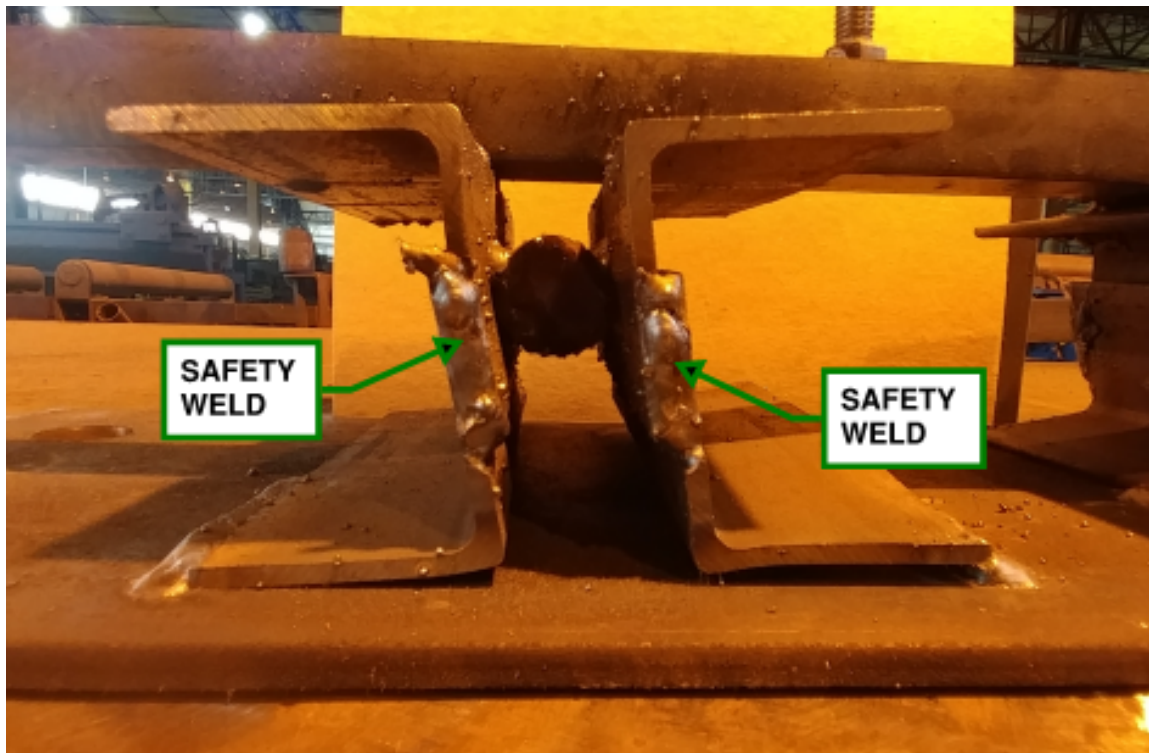


Figure 3-11 - Safety Weld on Lapped Configuration Joist Seats

3.6 Test Procedure

Each specimen pair was placed into the test table and loaded following this procedure:

- 1) Specimens were loaded on to the specimen platform and secured with 4, 1 in. A490 bolts tightened initially hand tight.
- 2) The load transfer bar was attached to the specimen continuity bar with a single $\frac{3}{4}$ in. A325 bolt tightened hand tight.
- 3) The load cells were advanced until 150 pounds of pressure were recorded then slowly relaxed to pull the “slack” out of the system and ensure that all bearing connections were active.
- 4) The 4, 1 in. A490 bolts securing the specimen to the specimen platform were tightened snug tight.
- 5) The two bearing plate stiffeners were installed and the eight, 1.5 in. A325 bolts were tightened snug tight.
- 6) The data acquisition system was checked and zeroed.
- 7) The hydraulic cylinder was advanced, adding pressure via a manual hand pump until ultimate failure was observed.
- 8) As such point that failure was observed, the hydraulic cylinder was fully relaxed and final data was recorded.

Ultimate failure was defined as the observation of any of the following mechanisms:

- 1) Failure of the bearing weld between the joist’s seat and the bearing plate;

- 2) Failure of an internal seat weld, causing a full loss of strength; or,
- 3) Material fracture of the bearing angles, bearing plates, or other element of the specimen, resulting in full loss of strength.

Chapter 4 – Results

4.1 Introduction

The intent of these experiments was to measure the strength of steel joist seats subjected to rollover forces as well as to identify the controlling mechanisms. Points of interest included first yield of the tension side bearing angle and the point of ultimate failure.

This section discusses the qualitative and quantitative test results from the fifteen specimens. The qualitative test results include observed behaviors of the specimens and their failure mechanisms, as well as unique events in each test. The quantitative test results are the estimated elastic, and ultimate limits states based on the collected data.

4.2 Qualitative Test Results

During the fifteen tests, there was a common sequence of mechanisms that eventually led to the ultimate failure of the joist seat. For specimens that deviated from this sequence, it is clear that other imperfections during fabrication were the cause. Such cases will be addressed later in this chapter. The typical sequence is described below.

Initially the joist seats exhibited a very stiff and linear response to the lateral loading until there was yielding of the tension side bearing angle and a plastic hinge began to form. The shape of the plastic hinge in the bearing angle resembles the yield lines drawn

in Green and Sputo (2002) as seen in Figure 4-1. However, it should be noted that unlike the lines drawn in Green and Sputo (2002), which varied with the thickness of the bearing angles, the yield line was the same for all specimens. It started at the edge of the “k” dimension at the end of the seat, and then wrapped down to the toe at the opposite end of the bearing weld.



Figure 4-1 – Test 15155-A Yield Line Formed on the Tension Side Bearing Angle

As load was added, portions of the seat began to yield and stiffness continued to decrease. This resulted in significant lateral deflections. During this time the torsional effects of a non-symmetrical bearing weld became apparent and the seat began to experience unsymmetrical deformations and rotations. As loading increased, the seat exhibited a new comparably flexible response until failure of the tension side bearing

weld of one or both joist seats. For many of the seats, the torsional aspect of the configuration caused the weld to be slowly torn back as can be seen in Figure 4-2, reducing the ultimate strength of the weld until rupture occurred.



Figure 4-2 – Bearing Weld Tear on 15155-A

4.3 Individual Specimen Results

4.3.1 Test Configuration 20250

All specimens from configuration 20250 followed the common sequence of mechanisms to failure. However, Specimen 20250-A exhibited a stiffer initial response as shown in Figure 4-3, and a higher ultimate strength. Further investigation showed that the internal seat weld connecting the bearing angles to the top chord had been undersized to roughly three inches on specimens 20250-B and 20250-C. 20250-A was

likely a better representation of the actual capacity of the typical seat of its configuration because its internal weld was the typical length of four inches. Note that some of the data from specimen 20250-B was lost and a simple linear interpolation was used to estimate the response from the last recorded data point to ultimate strength.

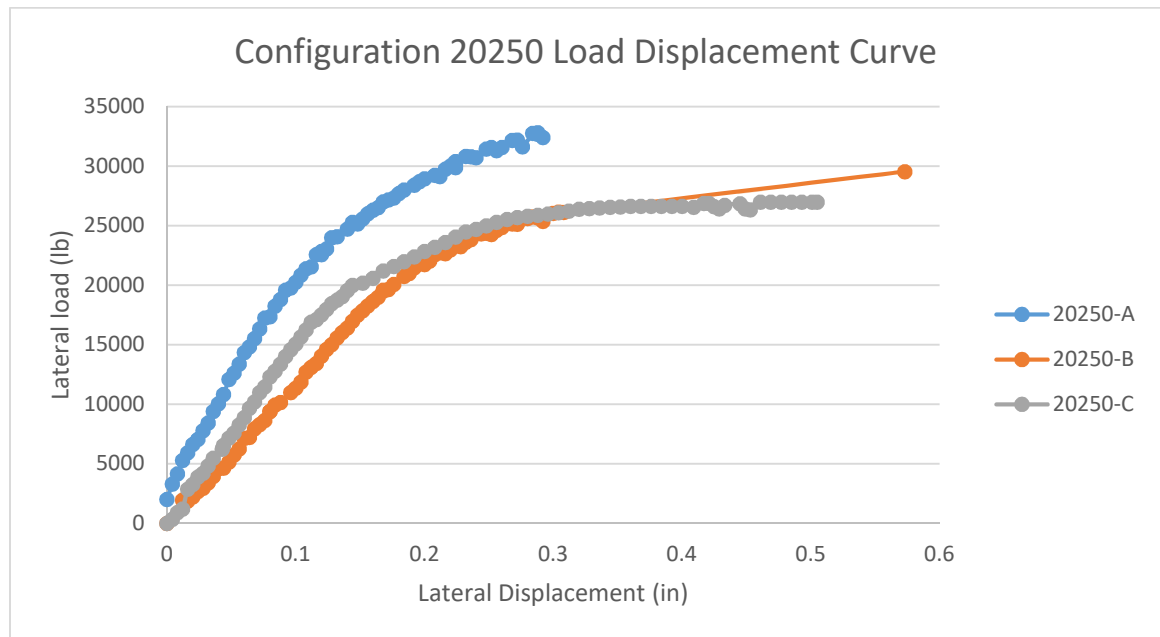


Figure 4-3 - Configuration 20250 Load Displacement Curve

4.3.2 Test Configuration 20188

All specimens from configuration 20188 followed the common sequence of mechanisms to failure. Specimen 20188-B experienced minor cracking in the internal seat weld connecting the bearings angles to the top chords, which caused a local drop in strength as seen in Figure 4-4. This did not seem to impact on the ultimate capacity of the seat.

Specimen 20188-C reached slightly higher ultimate load. After reaching this high point, the torsional effects began tearing the bearing weld of both seats, creating a relaxing effect as the seat deflected more until the weld ruptured. This can be seen in Figure 4-5 by the large deflections of the joist seat at the edges of the bearing seat.

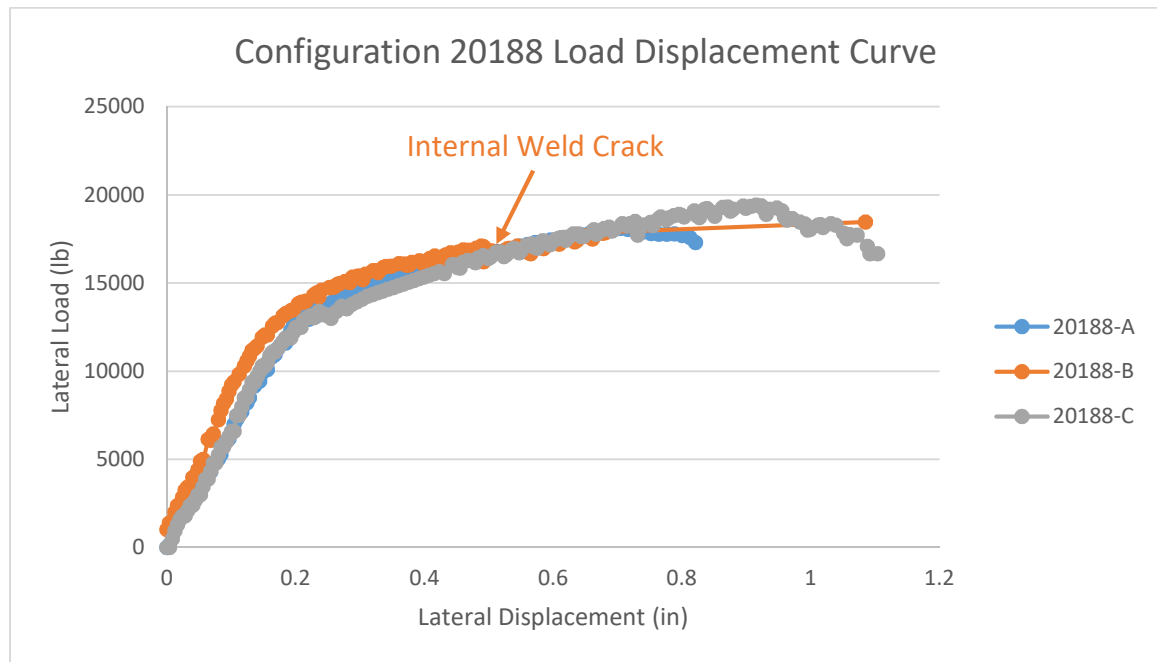


Figure 4-4 - Configuration 20188 Load Displacement Curves



Figure 4-5 - Specimen 20188-C After Failure

4.3.3 Test Configuration 20163

All specimens from configuration 20163 followed the common sequence of mechanisms to failure. However, all specimens exhibited different initial stiffness before the normal elastic modulus was realized. This was most present on specimen 20163-A. Specimen 20163-B experienced minor cracking in the internal seat weld connecting the bearings angles to the top chords, which caused a local drop in strength as seen in Figure 4-6. Unlike specimen 20188-B, it appears that specimen 20163-B's ultimate capacity was notably affected by the internal weld fracture.

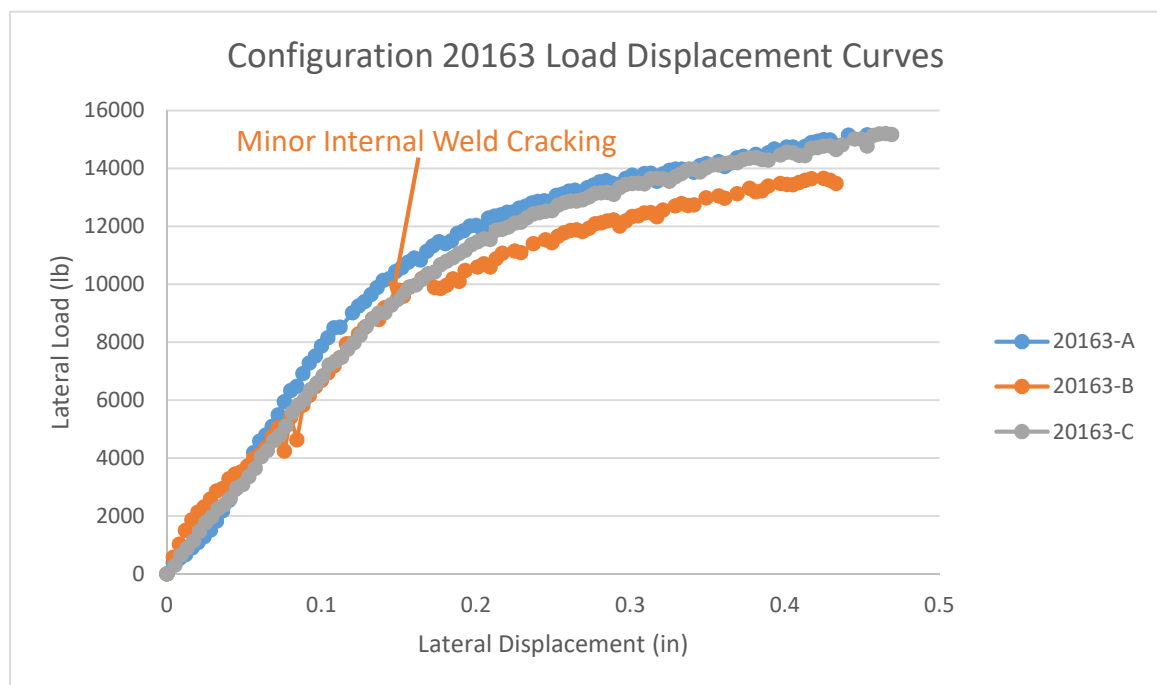


Figure 4-6 - Configuration 20163 Load Displacement Curves

4.3.4 Test Configuration 15155

All specimens from configuration 15155 followed the common sequence of mechanisms to failure as seen in Figure 4-7. Note there is no data for specimen 15155-A due to a failure of the data acquisition system. Similar to 20188-C, the 15155 configuration specimens had tearing of the bearing welds due to the torsion in the seat, which reduced the ultimate strength of the seat and resulted in larger displacements. This was seen on all specimens except specimen 15155-A, which had a sudden combined weld and base metal rupture.

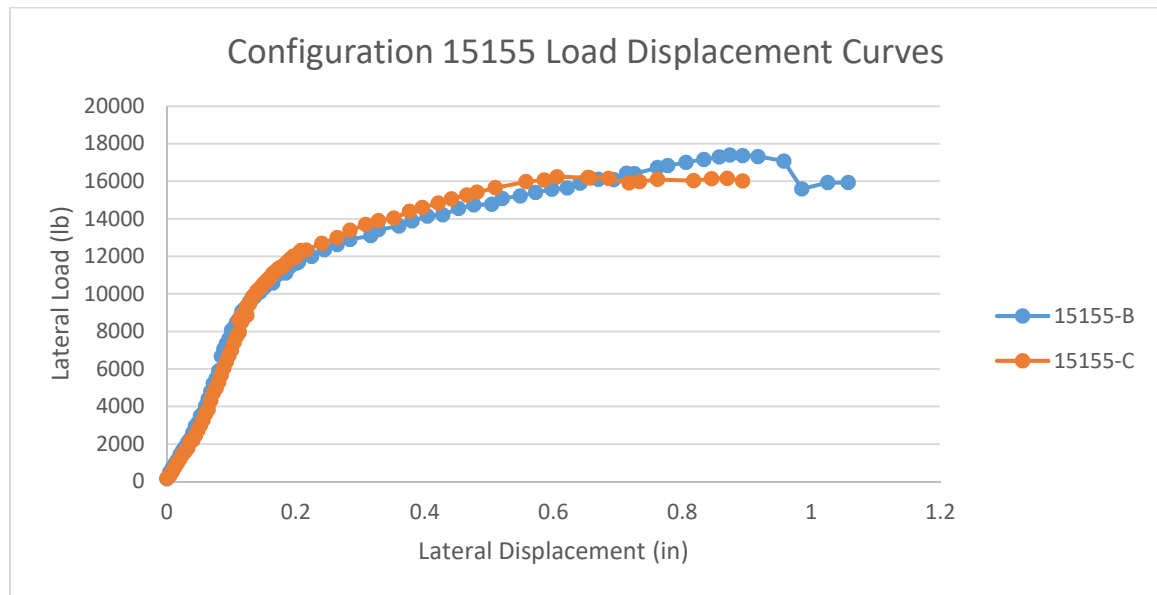


Figure 4-7 - Configuration 15155 Load Displacement Curves

4.3.5 Test Configuration 15113

All specimens from seat configuration 15113 followed the common sequence of mechanisms to failure. However, it is interesting that after exhibiting very similar initial stiffness in the elastic range, all three specimens exhibited different stiffness in the

inelastic range. However, unlike the specimens in configuration 20250, the difference in stiffness in the inelastic region did not have an effect on the ultimate capacity, which was almost identical for all three specimens. Note that part of the data from specimen 15113-A was lost.

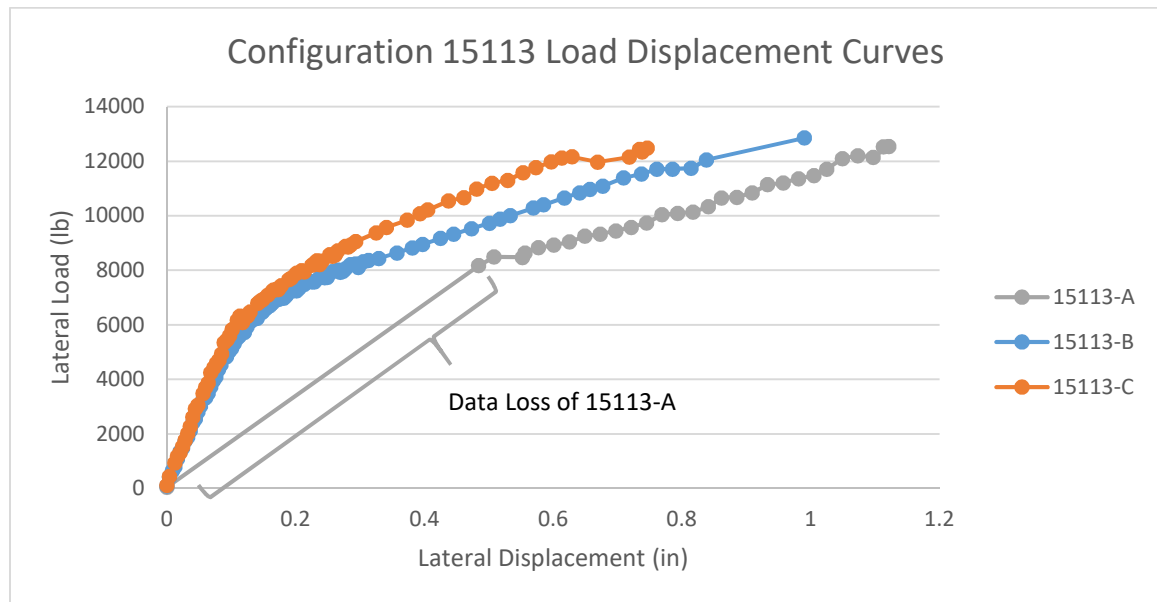


Figure 4-8 - Configuration 15113 Load Displacement Curves

4.4 Quantitative Results

The primary goal of the experiments was to obtain records of the initial yield and ultimate capacities of joist seats subjected to rollover forces. This data would help verify the development of a more accurate method for estimating the capacity of seats under these conditions. This section will focus on estimating the capacity of the tested seats at each of these mechanisms based on the collected experimental data.

The method for determining first yield of the joist seat, or the elastic limit of the specimen, was the five percent offset method. Using this method, a line is drawn

representing the modulus of elasticity by matching a trend line to the most consistent section of the initial linear response of the specimen. Yield is then determined as the point when the load displacement curve deviates more than five percent from this elastic line. An example of this application can be seen in Figure 4-9. The results of this analysis can be seen in Table 4-1.

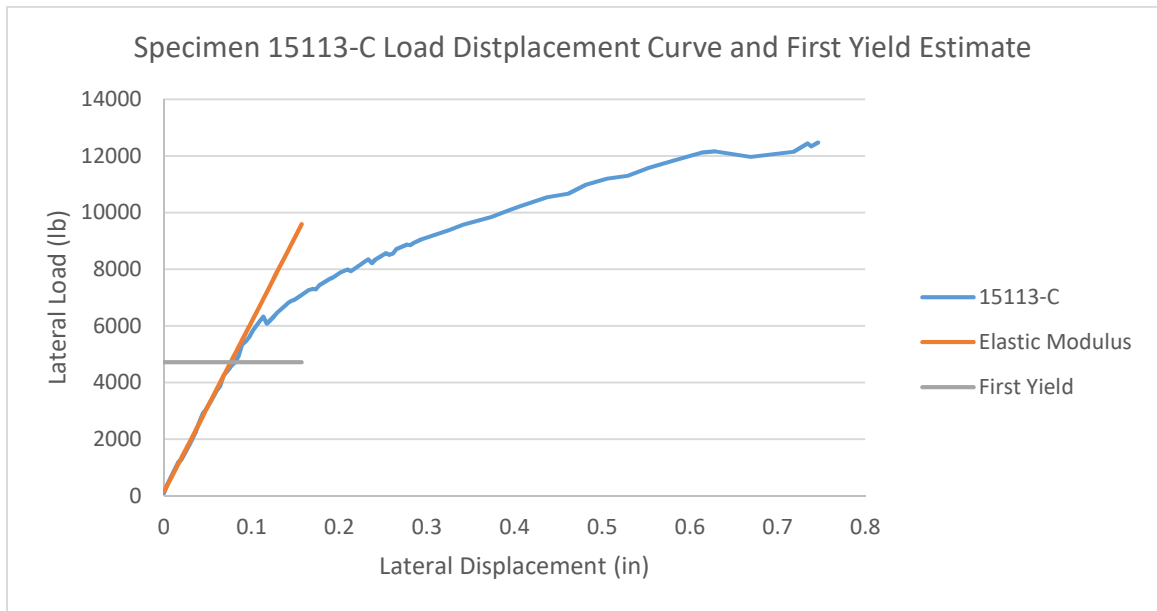


Figure 4-9 - Example of an Modulus of Elasticity Line Matched to a Load Displacement Curve to Determine the First Yield Point

Table 4-1 - First Yield and Ultimate Loading Recorded from Experiments

Specimen Designation	Modulus of Elasticity	First Yield		Ultimate		Percent Deviation from Average (%)
		Load (lb)	Disp. (in)	Load (lb)	Disp. (in)	
20250-A	196,582	19,787	0.096	32,836	0.292	-0.28%
20250-B	120,567	20,990	0.188	29,554	0.573	5.78%
20250-C	152,015	18,752	0.132	26,982	0.505	-5.50%
20188-A	70,094	11,612	0.184	18,115	0.821	2.44%
20188-B	84,403	11,293	0.136	18,469	1.085	-0.37%
20188-C	74,913	11,101	0.168	18,383	1.136	-2.07%
20163-A	68,135	8,786	0.137	13,659	0.441	1.00%
20163-B	93,395	8,517	0.112	16,118	0.601	-2.10%
20163-C	72,986	8,795	0.133	15,204	0.469	1.10%
15155-A	-	-	-	16,917	0.958	
15155-B	105,508	8,507	0.108	15,934	1.057	-1.95%
15155-C	87,144	8,845	0.128	16,168	0.909	1.95%
15113-A	-	-	-	12,531	1.639	
15113-B	53,731	4,832	0.092	12,863	0.99	1.20%
15113-C	60,090	4,717	0.081	12,487	0.746	-1.20%

When looking at these results, it is very interesting to note that while the modulus of elasticity may vary widely between specimens of the same configuration, the first yield strengths and the ultimate strengths were very similar, with much smaller deviations. Table 4-2 demonstrates to what extent this is the case. The normalized variance, variance of the sample divided by the average of the sample, of every load based data point is lower than the respective displacement and modulus data point.

Table 4-2 - Variation of Modulus of Elasticity, First Yield and Ultimate Loads and Displacements from Experimental Data

Specimen Configuration	Modulus of Elasticity	Variation at First Yield		Variation at Ultimate	
		Load	Disp.	Load	Disp.
20250	19.9%	4.6%	27.3%	8.0%	26.2%
20188	7.8%	1.9%	12.3%	0.8%	13.6%
20163	14.0%	1.5%	8.6%	6.8%	13.9%
15155	9.5%	1.9%	8.5%	2.6%	6.3%
15113	5.6%	1.2%	6.4%	1.3%	33.5%

Chapter 5 – Discussion

5.1 Introduction

The goal of this research was to identify the mechanisms controlling the strength of steel joist subjected to rollover forces in order to more accurately estimate their capacity. This section will discuss the findings of the research and experimentation and give commentary of plausible concepts for design.

5.2 Effects of Fabrication Quality

When initially loaded, the joist seats exhibited a short period of relatively inconstant stiffness, sometimes being stiffer than the actual elastic modulus, and sometimes more flexible. This was one of many different anomalies that were observed during testing that differed from the expected response. It would appear that many of these anomalies are caused by imperfections created during the fabrication process. The nature of welding in the fabrication process means that some elements are subjected to significant distortion due to uneven heating. This is particularly true of the bearing angles. This is very apparent when comparing the idealized sketch of a joist seat to one that has actually been fabricated in the shop, as can be seen in Figure 5-1.

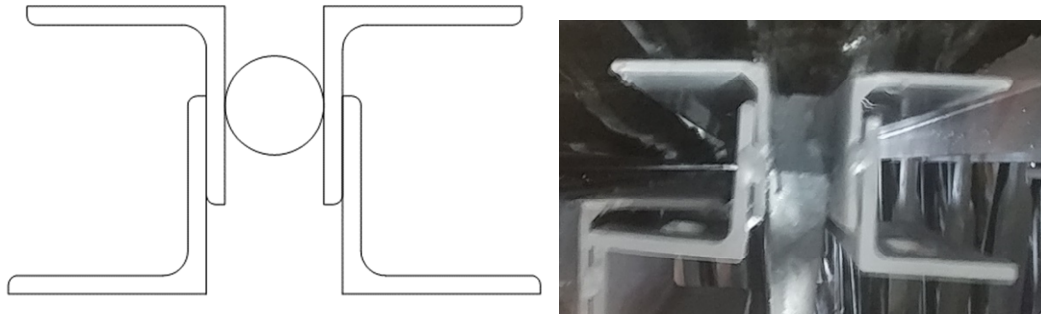


Figure 5-1 - Idealized Sketch of Joist Seat vs. the Manufactured Joist Seat

These distortions change the geometry, balance of loading, and contacts of the seats, which affects lateral and torsional stiffness, and capacity. However, it is not the goal of this report, or likely any report, to address the consequences of all potential fabrication fallacies. When addressing the primary failure mechanisms, this report will seek to ignore these small deviations when possible. While fabrication discrepancies are likely the cause for the large variances in stiffness and initial response, it does not appear that it had as significant of an effect on the overall capacity of the joist seats. So ignoring effects of fabrication on capacity is reasonable.

5.3 Overview of Statics

As discussed in the introduction of the report, there are two primary forces in the joist seat when subjected to rollover forces, shown in Figure 5-2. The first is the lateral rollover force " V " that is applied by an external element, typically a deck edge or the steel deck. The second is the couple, with forces " F_v ", that forms to resist the static moment that forms between the lateral rollover force and the support. The moment arm for the rollover force is simply the height of the joist seat, with the applied lateral load occurring at the top of the top chord, and the reaction occurring on the bottom of

the bearing angles. However, the moment arm for the resulting couple is more complex. It is certain that the negative reaction occurs at the tension's side bearing weld connecting the bearing angles to the support. However, the location of the positive reaction will vary depending on a number of factors including the size of the bearing angles, the chord gap, and the stiffness of the seat configuration, which is itself affected by a number of factors. The length of this moment arm is denoted as “m” and will be a point of interest in this chapter.

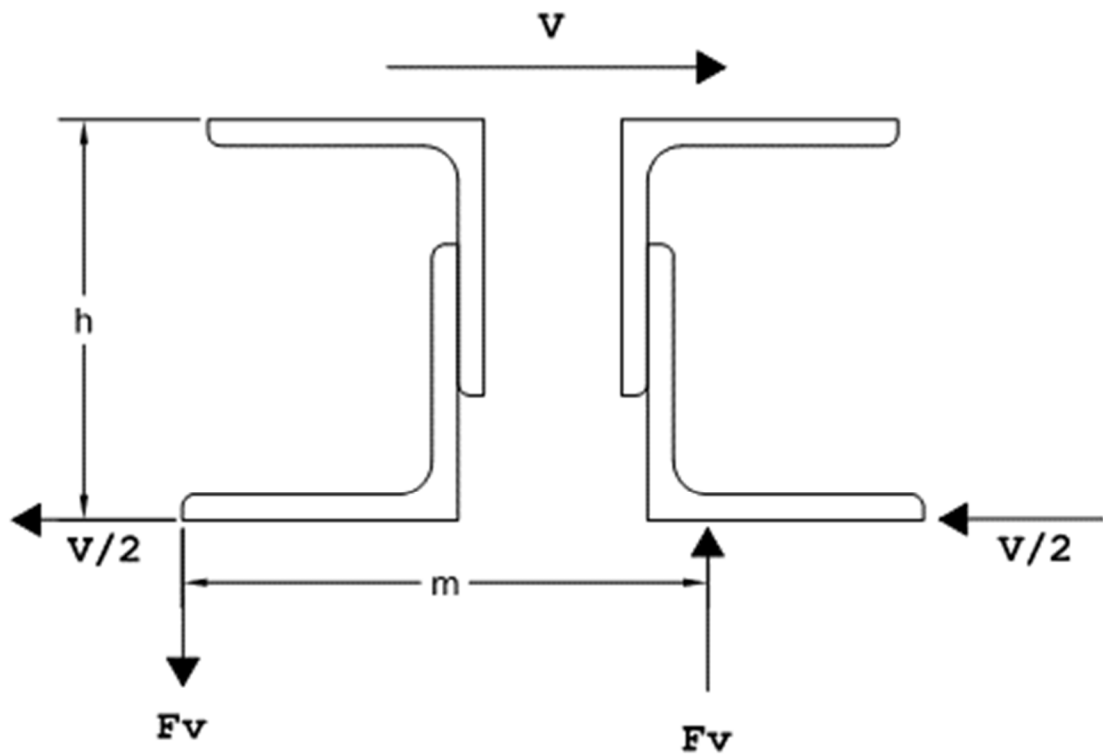


Figure 5-2 - Typical Statics of a Steel Joist Seat Subjected to Rollover Forces

5.4 Mechanisms

For all joist seats that were tested, there was a common sequence of mechanisms that eventually led to ultimate failure. From statics, these mechanisms can be separated into two stages: elastic and inelastic. These stages can be seen in the load displacement curves as shown in Figure 5-3.

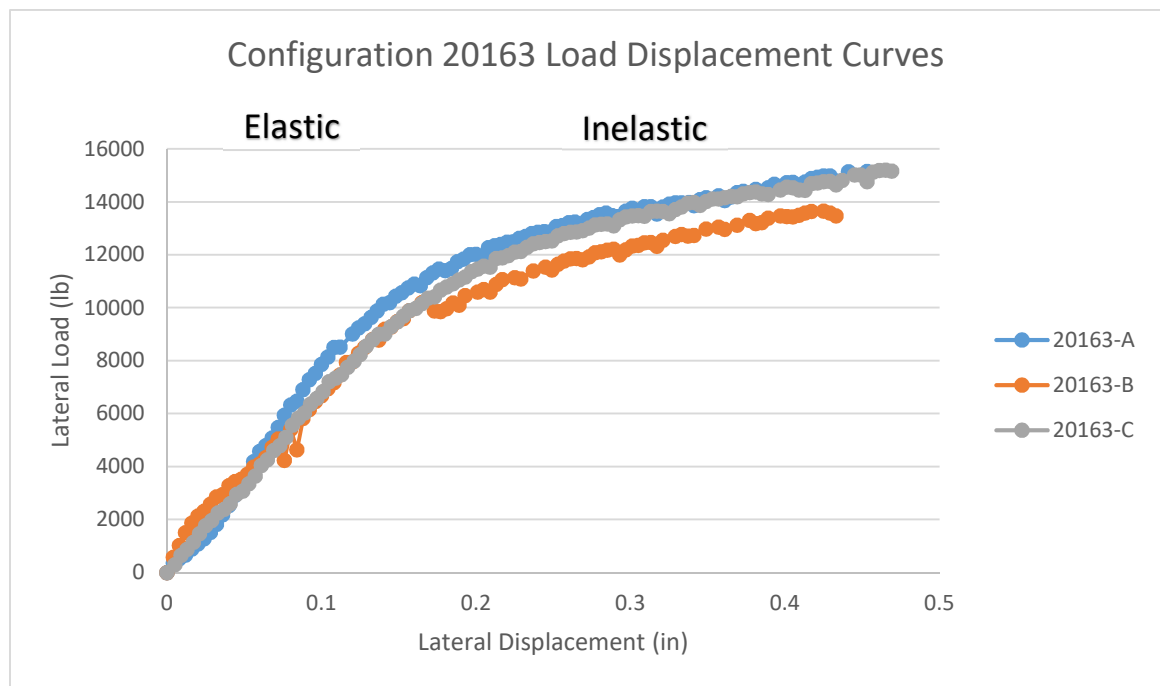


Figure 5-3 - The Two Mechanism Stages Shown on Experimental Data

During the elastic stage, the joist seat primarily exhibits a very stiff elastic response to loading until first yielding occurs in the tension side bearing angle. This yielding forms along a yield line similar to that observed in Green and Sputo (2002) as shown in Figure 5-4.



Figure 5-4 - Typical Observed Yield Line During Testing

Like Green and Sputo (2002), this yield line can be simplified, potentially as shown in a top down view of the tension side bearing angle in Figure 5-5, where the distance “a” is equal to 2.3 times the thickness of the bearing angle. It is also important to note that, during this stage, the presence of lateral forces in the tension side bearing seat have very little effect compared to the vertical forces, “ F_v ”, of the couple. This finding is extremely important, as it shows that the first yielding mechanism is similar for both rollover and uplift forces. This becomes very convenient when determining the capacity of joist seats under combined rollover and uplift conditions, which is more realistic to actual conditions experienced in the field.

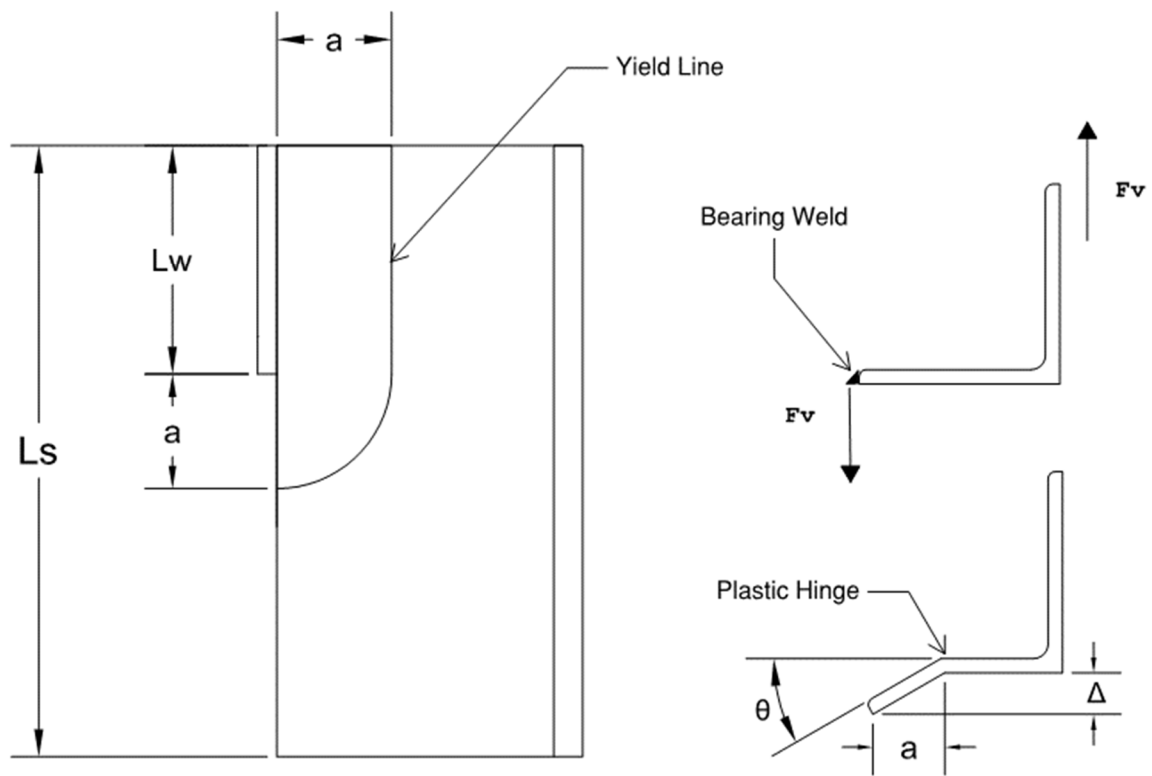


Figure 5-5 - Idealized Yield Line Based on Green and Sputo (2002)

During the inelastic stage, first yield has occurred in the tension side bearing angle and the plastic hinge begins to develop. As this continues, other portions of the seat will begin to yield as well, until the seat has formed plastic hinges throughout and begins to resemble a specimen from the Fisher et al. (2002) as shown in Figure 5-6 and idealized in Figure 5-7.



Figure 5-6 - Joist Seat After Failure due to Lateral Rollover Forces

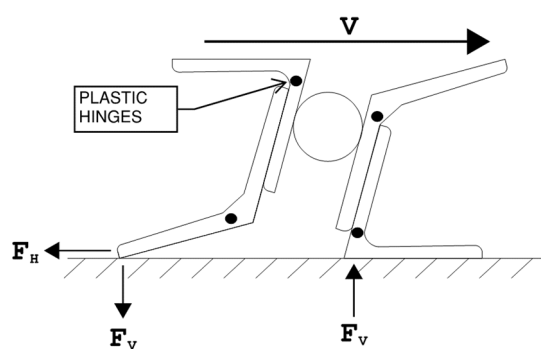


Figure 5-7 - Seat Appearance After Formation of Plastic Hinges in All Elements.

At this point, the seat will exhibit a consistent stiffness until failure of one element in rupture, or the more likely failure of the bearing weld in rupture. This stage is also where any torsion in the seat will have the greatest effect. The torsion will cause the

bearing weld to be unequally loaded near the middle of the seat and will cause it to tear apart, reducing the ultimate capacity of the weld until failure.

5.5 Performance in Each Stage

5.5.1 The Elastic Stage

The capacity of a joist seat during the Elastic Stage can be estimated by applying the yield line from Green and Sposito (2002) to the statics of a joist seat subjected to rollover as seen in Figure 5-8. The statics are similarly applied to the yield line equation such that

$$P_u = \frac{M_p L_{YL}}{a} \quad (5-1)$$

becomes

$$V_{yl} = \frac{M_p L_{YL}}{a} * \frac{m}{h}, \quad (5-2)$$

again where

M_p = Plastic moment capacity of the plate, per unit length of plate = $F_y S$

L_{YL} = Length of the yield line, the lesser of $(L_w + \pi a)$ and L_s

L_w = Length of anchorage weld

L_s = Length of the seat angle

F_y = Average 0.2% offset yield stress of the steel angle

S = Section modulus of unit length of plate which is $t^2 / 6$

t = Thickness of seat angle leg

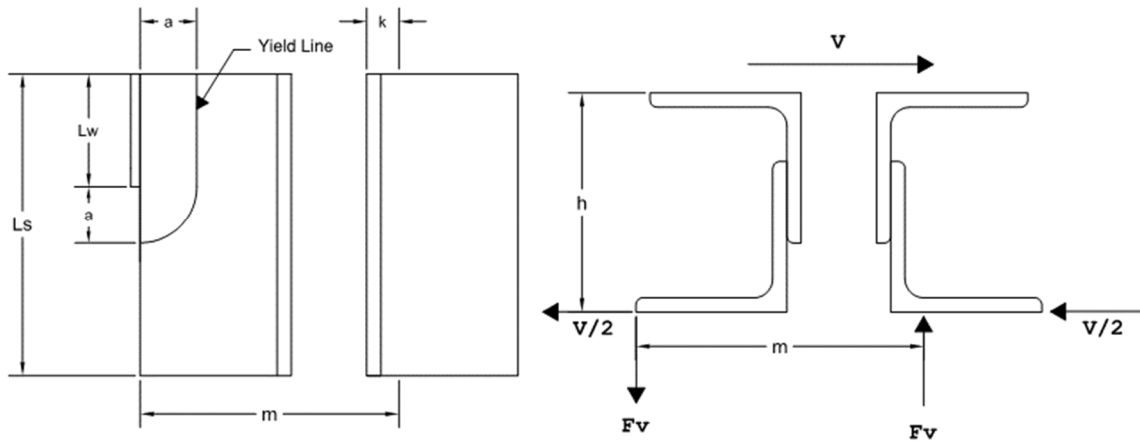


Figure 5-8 - Applying Green and Sputo (2002) Yield Line to Joist Seats Subjected to Rollover

As stated earlier in this report, behavior on the tension side is fairly certain based on statics. However, uncertainty on the compression side leads to many questions, namely the location of the compression reaction and the moment arm of the couple “m”. Table 5-1 contrasts the average experimental performance of each seat configuration at first yield with the theoretical capacity with different values of “m” with the compression reaction at the heel, the end of the k dimension, the Vulcraft Alabama location, and the toe of the compression angle.

Table 5-1 - Comparison of Likely Locations for the Compression Reaction

Specimen Configuration	Thickness (in)	Average First Yield Load (lb)	Estimated Capacity With Compression Reaction at			
			Heel (lb)	K dimension (lb)	VAL (lb)	Toe (lb)
20250	0.25	19,843	8,344	9,387	10,057	13,111
20188	0.188	11,335	5,556	6,173	6,687	8,848
20163	0.163	8,699	4,766	4,881	5,318	7,085
15155	0.155	8,676	4,766	5,212	5,625	7,310
15113	0.113	4,775	3,331	3,621	3,934	5,163

It would seem that from this data, the best assumption is that during the elastic stage, the compression reaction is located at the toe of the compression angle. However, even located there, at the least conservative location, the model underestimated the first yield capacity of all joist seats except the 152 seat configuration with 0.113-inch-thick bearing angles. Once more, the degree of error as seen in Table 5-2 scales quadratically with thickness, which indicates drawing the yield line similar to Green and Sposito (2002) may not be correct. This can be seen by graphing the data as shown in Figure 5-9, with the experimental average yield plotted with points and the estimated first yield as predicated with the Green and Sposito (2002) yield line geometry drawn with the dashed line. The shapes created by each do not appear to be compatible. Both curves follow a quadratic line. However, while the experimental data is nearly tangent with the origin, the estimation using Green and Sposito (2002) is not as it exhibits an initial slope.

Table 5-2 - Deviation of Observed First Yield Strength vs. First Yield Strength Estimated with Application of Green and Sputo (2002)

Specimen Configuration	Average First Yield Load (lb)	Estimated Elastic Strength	Percent Deviation
20250	19,843	13,111	-34%
20188	11,335	8,848	-22%
20163	8,699	7,085	-19%
15155	8,676	7,310	-16%
15113	4,775	5,163	8%

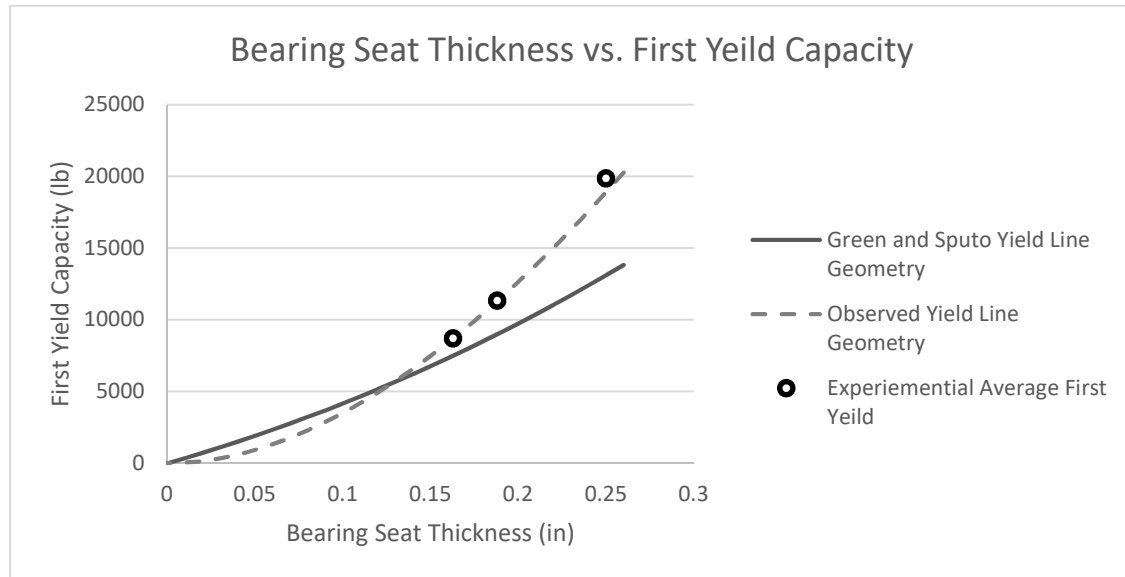


Figure 5-9 - Bearing Seat Thickness vs. Elastic Limit

This makes sense, as it was observed that unlike the yield line in Green and Sputo (2002) which varied with the thickness of the bearing seat, the yield line observed in these experiments was consistent across all thicknesses. While using the Green and Sputo (2002) yield line, the elastic limit “ V_{ly} ” correlated to $t^2 + t$. According to the data, the elastic limit “ V_{ly} ” correlates to t^2 only. The yield line would instead be drawn

from some distance “b” along the edge of the seat, near the k dimension, to the toe of the bearing angle at the opposite end of the bearing weld as shown in Figure 5-10.

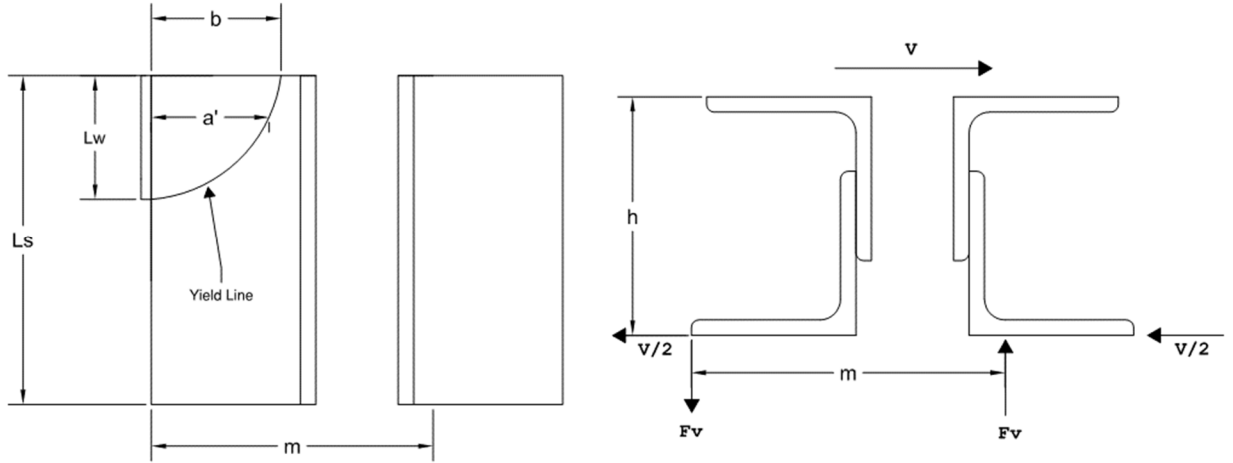


Figure 5-10 - Yield Line Based on Experimental Data

With the yield line idealized as a quarter of a simple ellipse as shown, the yield line theory expressed by Green and Sputo (2002) can be adapted to better predict the joist seat response. The “a” dimension is used by Green and Sputo (2002) to express the moment arm between the reaction at the bearing weld and the yield line. It written as

$$M = Fv * a, \quad (5-3)$$

where

M = design moment across the yield line due to the vertical reaction at the bearing weld

Fv = vertical reaction at the bearing weld

σ = unit stress due to the vertical reaction along the bearing weld

Lw = length of the bearing weld

b = distance from the toe of the bearing angle to the start of the yield line

h = the height of the bearing seat

m = the moment arm between the couple force reactions.

With the new geometry of the yield line, this moment arm is not constant so “a” must be adjusted. The demand moment along the yield line is the unit force at the bearing weld multiplied by the perpendicular distance from the bearing weld to the yield line, denoted in Figure 5-10 as “a’”. Integrating along the length of the weld like so,

$$M = \int (\sigma * a') dLw, \quad (5-4)$$

yields the full moment demand across the yield line and can be used to define “a”. The unit stress can be idealized as the total reaction at the bearing weld divided by the length of the bearing weld,

$$\sigma = Fv/Lw. \quad (5-5)$$

and “a’” can be defined by the equation of a simple ellipse,

$$a' = b \sqrt{1 - \frac{x^2}{Lw}}, \quad (5-6)$$

where x is defined along the length of Lw. Substituting into equation 5-4,

$$M = \frac{Fv}{Lw} \int b \sqrt{1 - \frac{x^2}{Lw}} dx. \quad (5-7)$$

The integral of “a’” equal to one fourth the area of the simple ellipse, so equation 5-7 can be simplified to,

$$M = \frac{Fv}{Lw} * \frac{(b * Lw * \pi)}{4}, \quad (5-8)$$

and further to

$$M = Fv * \frac{b\pi}{4}. \quad (5-9)$$

This shows that for the new yield line geometry, “a” in equation 5-3 is

$$a = b\pi/4. \quad (5-10)$$

The value of b could be estimated by fitting the curve to the experimental data similarly to that done by Green and Sposito (2002). This would result in a simplified and conservative estimation of the response in the elastic stage.

Utilizing the data from the experiments,

$$b = 0.13 * L_{leg} + 0.5 * t \quad (5-11)$$

results in a relatively reliable and conservative model for predicting the capacity of each of the joist seat assemblies, as can be seen in Table 5-3. However, this representation is only presented to show that such a relationship is plausible. Further testing across a larger range of bearing angle sizes would need to be conducted to produce an industry ready model with confidence.

Table 5-3 - Experimental vs. Theoretical First Yield Capacity Utilizing Adjusted Yield Line Model

Experimental First Yield		Estimated First Yield (lb)
Load (lb)	Disp. (in)	
19,787	0.096	18,911
20,990	0.188	18,911
18,752	0.132	19,807
11,612	0.184	11,126
11,293	0.136	11,126
11,101	0.168	11,126
8,786	0.137	8,165
8,517	0.112	8,165
8,795	0.133	7,757
-	-	9,635
8,507	0.108	10,125
8,845	0.128	10,125
-	-	5,929
4,832	0.092	5,929
4,717	0.081	5,641

5.5.2 The Inelastic Stage

Response during the inelastic stage is defined by yielding and formation of plastic hinges. During this stage the vertical reaction at the bearing weld is greater than what the bearing seat can carry in flexure across the yield line. This is possible because the tension side horizontal leg is deformed to allow a tension force in the member to cover the additional vertical component of the reaction as seen in Figure 5-11.

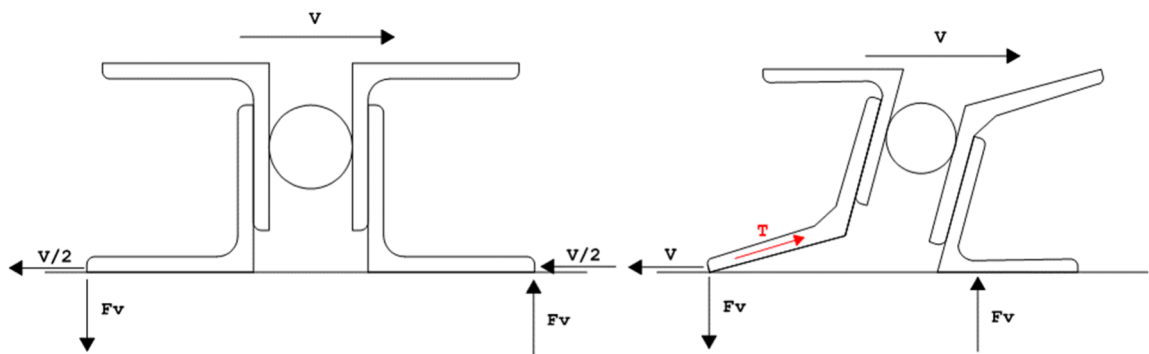


Figure 5-11 - Tension Component Forms as Bearing Angle Deforms

In all tests, the ultimate failure was at the bearing weld on the tension side. This is well explained by the observed statics. All internal welds have a larger capacity due to their longer length than the bearing weld. The only other ultimate failure mode would be via rupture in the bearing angles. However, rupture will not occur due to flexure, as the tension side bearing angle will simply continue to deform, carrying more of the vertical components of the reaction in tension. Eventually, the full load of both lateral and vertical reactions would be carried in tension. This would mean that a material rupture in the bearing angles could only occur due to gross section rupture. In industry, this is not likely to occur as the angle material in the bearing seats will always be 50ksi

or greater due to code requirements, and the weld material will not exceed 80ksi due to field welding practices during erection. Therefore, the ultimate failure mode would most certainly be due to a rupture in the bearing weld.

This failure can be estimated based on the initial ultimate strength method proposed by Fisher et al. (2002) as shown in Table 5-4. Simple statics show that the stress across the effective throat of the tension side bearing weld “P” is

$$P = \sqrt{V^2 + Fv^2} \quad (5-12)$$

or the combined force of the full lateral reaction and the induced vertical tension reaction. Note that “Fv” can be set to

$$Fv = V * h/m \quad (5-13)$$

to put all variables in terms of V. The capacity of the weld “R” is

$$R = 0.6 * F_{exx} * \sqrt{2} * t * Lw, \quad (5-14)$$

where

F_{exx} = the tensile strength of the weld material, assumed to be 70ksi

t = the thickness of the bearing angles

L_w = the length of the bearing weld

The maximum allowable lateral force can be found by setting equation 5-12 equal to equation 5-14, substituting where applicable, and then solving for “V”. The result is

$$V = \frac{0.6 * F_{exx} * \sqrt{2} * t * Lw}{\sqrt{1 + \frac{h^2}{m^2}}}. \quad (5-15)$$

Determining the location of the compression reaction becomes more difficult in the inelastic stage due to the formation of the plastic hinges. Therefore, it is best to assume

that the compression reaction is located at the end of the k dimension on the compression side bearing angle. Experimental data shows this to be an accurate, but slightly conservative, assumption. However, it should be noted that due to torsional effects, this full capacity is not likely to be achieved. The imbalanced loading will cause the bearing weld to tear at the later stages of the inelastic stage, reducing the ultimate capacity of the bearing weld until rupture.

Table 5-4 - Experimental vs. Theoretical Ultimate Capacities

Specimen Designation	Thickness (in)	Experimental Ultimate		Fisher et al. (2002) Ultimate Strength
		Load (lb)	Disp. (in)	
20250-A	0.25	32,836	0.292	32,499
20250-B	0.25	29,554	0.573	32,499
20250-C	0.25	26,982	0.505	34,124
20188-A	0.188	18,115	0.821	24,372
20188-B	0.188	18,469	1.085	24,372
20188-C	0.188	18,383	1.136	24,372
20-163-A	0.163	13,659	0.441	19,063
20163-B	0.163	16,118	0.601	19,063
20163-C	0.163	15,204	0.469	18,060
15155-A	0.155	16,917	0.958	19,222
15155-B	0.155	15,934	1.057	20,233
15155-C	0.155	16,168	0.909	20,233
15113-A	0.113	12,531	1.639	14,859
15113-B	0.113	12,863	0.99	14,859
15113-C	0.113	12,487	0.746	14,116

5.6 Summary

Across the 15 specimen tests, specific section properties of the seat materials were varied, but the failure mechanisms remained consistent. Analyzing the resulting load

displacement curves showed two stages of mechanisms that ultimately led the rupture of the bearing weld on the tension side of the joist seat. Applying concepts from the Fisher et al. (2002) and Green and Sposito (2002) to the yield line observed in the experiments showed a plausible method for predicting capacity.

Chapter 6 – Summary and Conclusions

6.1 Introduction

The goal of this study was to document the current methods and theories for designing steel joist seats subjected to rollover forces, and apply that body of knowledge to explore a new design method that more closely matches industry practices and real world mechanisms. This chapter will briefly review the important aspects of the study, present the important conclusions, and make recommendations for future studies to further the body of knowledge on this topic.

6.2 Summary of Existing Body of Knowledge and Design Methods

There are several existing methods that have been developed from a number of experimental studies. However, there were several discrepancies with many of the experimental setups that deviated from real world conditions. Most notably were unrealistic loading mechanisms and non-standard bearing weld lengths and placements.

Regarding loading mechanisms, before Doyle (2010), tests were conducted with only single specimens rather than seat pairs, which allowed the seats to unrealistically cant due to the lack of a rigid element connecting to the top chord. This would have significantly reduced the apparent capacity of the joist seats.

Regarding bearing weld length and placement, most studies were conducted with bearing welds along the full length of the joist seat, when in reality the Steel Joist

Institute only requires two and a half inches of bearing weld for K-Series joists, and four inches for LH series joists. Additionally, it was important to check the worst case scenario, with the weld located at the end of the joist seat, rather than centered on it.

The existing methods presented by Fisher et al. (2002) were the most notable that had been developed, and were most widely used. However, their Elastic Strength Method was very conservative compared to actual experimental strength. The existing method for designing steel joist seats for uplift, as presented by Green and Sposito (2002), might be applied to the Elastic Strength Method to more accurately predict the joist seat failure mechanism and capacity

6.3 Conclusions

Addressing the aforementioned concerns by testing joist seats in series as done in Doyle (2010), and with the correct bearing weld length at the critical location, the experimental series conducted in this study yielded positive and consistent results. The data from these experiments was used to show that the application of theories from Green and Sposito (2002) and Fisher et al. (2002) could yield a plausible model to predict the elastic and ultimate strengths of the test specimens.

6.4 Location of the Bearing Weld

A key element to this field of testing was size and location of the bearing weld. As was identified in this report, the location of the bearing weld can have a significant impact on the failure mechanisms and thus the rollover capacity of the joist seats. However, there is no requirement in code specifying the location of the bearing weld, only the fillet size and length. Therefore, the bearing weld can be located anywhere along the length of the bearing seat. This flexibility in code could be a significant barrier to creating a simple design method for industry, as the final location of the bearing weld would be unknown to the specifier and joist manufacturer at the time of design. Therefore, it may be prudent for the governing bodies, namely the Steel Joist Institute, to expand the governing codes to specify a more specific location of the bearing weld.

6.5 Future Research

While the experiments in this research yielded positive results, they are certainly not sufficient to justify a new industry model. More tests with specimens across more bearing seat thicknesses would be required to experimentally match such a method as done by Green and Sputo (2002). Additionally, although the yield line theory does better represent the failure mechanisms, it cannot completely describe the real world phenomena. Adequately predicting a response and fully explaining a response are not the same. Further testing and exploration into the effect of the seat stiffness, the location of the compression reaction, and even the properties of the yield line, with

more precise analytical modeling is suggested. However, given the small body of knowledge due to the specificity of this topic, any new data to shore up and refine existing models would help grow the confidence of the design community.

References

Abreu, J. C. B., R. D. Ziemian. 2017. "Computer Simulation of Joist Seat Rollover - Phase 1." unpublished, Bucknell University and The Steel Joist Institute.

Doyle, C. G., 2010. *Behavior of Open Web Steel Joist Seats Subjected to Lateral Loads*.

Villanova University.

Fisher, J. M., M. A. West, J. P. Van de Pas. 2002. Designing with Vulcraft Steel Joists, Joist Girders and Steel Deck 2 ed. Nucor Corporation.

Green, P. S., T. Sputo. 2004. *Uplift Capacity of K-Series Open Web Steel Joist Seats*.

American Society of Steel Construction.

McConnell, L., G. Watts. 2010. "Rollover Capacity of Open Web Steel Joists."

unpublished, Fort Payne, Alabama: Vulcraft Alabama.

SJI (Steel Joist Institute). 2017. *44th Edition Standard Specifications Load Tables and Weight Tables for Steel Joists and Joist Girders*. United States of America